3

Thermodynamics background

3.1 The properties of water and ions *page* 64
3.1.1 The structure of water 64
3.1.2 Water–ion interactions 68
3.2 Ion–ion interactions and activity coefficients 70
3.2.1 Activity–ionic strength relations 70
3.2.2 The mean salt method 71
3.3 Thermodynamic basics 73
3.3.1 Free energy change during reaction 74
3.3.2 Thermodynamic equilibrium 75
3.4 Equilibrium constraints on chemical activities 77
3.4.1 Speciation of ions in seawater 77
3.4.2 Equilibrium among coexisting phases: the phase rule 81
3.4.3 Solid–solution equilibrium: $CaCO_3$ 82
3.4.4 Solid–solution adsorption reactions 83
3.4.5 Gas equilibrium between the air and water 85
3.5 Redox reaction basics 89
3.5.1 The standard electrode potential, E_h^0, and p*e* 89
3.5.2 Environmental redox reactions 94
Table 3A1.1 Solubilities of the major atmospheric gases 98
References 99

One of the great advantages of the chemical perspective on ocean processes is the ability to predict whether specific reactions between molecules and ions might occur in aqueous media. Given the extreme complexity of natural systems, this type of fundamental constraint is invaluable. Such predictions are based on concepts and energetic information that have been painstakingly generated over the past several centuries and assembled into the discipline known as thermodynamics. The purpose of this chapter is to present an introduction to the properties of water and ions, and the basic concepts of the thermodynamics of chemical reactions. Rather than cover the breadth of thermodynamics, we seek to demonstrate the

Downloaded from https://www.cambridge.org/core. University of Hawaii at Manoa Library, on 09 Feb 2021 at 20:24:02, subject to the Cambridge Core terms of use, available at https://www.cambridge.org/core/terms. https://doi.org/10.1017/CBO9780511793202.004

applications of free energy to the prediction of equilibrium distributions of chemical species among gaseous, liquid, and solid phases. The goal is to establish the conceptual foundation and tools that can be applied to the following chapters on ocean processes.

3.1 The properties of water and ions

3.1.1 The structure of water

Water accounts for approximately 96.5 mass percent of seawater. The innate characteristics of water affect almost all the properties of the ocean (e.g. density, salinity, and gas solubility) and the processes (e.g. circulation, heat exchange, chemical reactions, and biochemical transformations) that occur within it. Water is so much a part of our world and daily lives that it is easy to overlook how unusual this substance is in its physical and chemical properties. A major source of this uniqueness originates at the molecular level from the much greater affinity (electronegativity) of oxygen versus hydrogen for shared electrons. In the two covalent bonds of an H_2O molecule, oxygen attracts the bulk of the electron density it shares with hydrogen and thereby acquires a partial negative charge that is redistributed into its two opposite non-bonding electron pairs (Fig. 3.1). As a result, each of the hydrogen atoms linked in the two bonding orbitals exhibits a partial positive charge. Because of the tetrahedral orientation of the four orbitals about the central oxygen, symmetric cancellation of this unequal electron distribution is not possible within individual H_2O molecules. Each H_2O molecule therefore exhibits a net separation of charge in space (Fig. 3.1), which is referred to as a *dipole*. Because the two electron pairs in the non-bonding orbitals about the oxygen atom are attracted primarily by the oxygen nucleus, their electron densities are more expansive, resulting in a repulsive force on the bonding orbitals that causes a bond angle compression. The H–O–H bond angle is compressed from the value for a perfect tetrahedron (109.5°) to 104.5°.

This unequal distribution of electronic charge within the H_2O molecule has huge ramifications for how these molecules interact and react. As a result of their polarity, H_2O molecules orient in solution in such a way as to minimize the proximity of like partial charges by (on average) turning hydrogens toward oxygens of neighboring molecules. Adjacent H_2O molecules undergo an additional form of intermolecular interaction known as *hydrogen bonding*, which is unique to molecules having hydrogen bonded directly to highly electronegative elements such as N, O, F and occasionally Cl. Hydrogen bonding can be thought of as an intermolecular attraction of the hydrogen atoms of water molecules. The hydrogen atoms of each individual water molecule interact along an O–H bond that is aligned with one of the two non-bonding orbitals of the oxygen in an adjacent H_2O molecule. Hydrogen bonds are weaker than ordinary intramolecular bonds but are generally the strongest type of

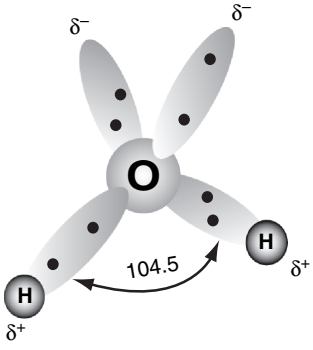


Figure 3.1. The three-dimensional structure of a water molecule. The sphere in the middle represents the oxygen atom and the dark circles are hydrogen atoms. Ovals represent electron orbitals of the outer shell electrons; δs indicate net charges.

Downloaded from https://www.cambridge.org/core. University of Hawaii at Manoa Library, on 09 Feb 2021 at 20:24:02, subject to the Cambridge Core terms of use, available at https://www.cambridge.org/core/terms. https://doi.org/10.1017/CBO9780511793202.004

intermolecular attraction. The resulting intermolecular interaction has a characteristic distance of 1.8 Angstroms ($1\,\text{Å} = 10^{-10}\,\text{cm}$) between the oxygen of one water molecule and the hydrogen of an adjacent water molecule and exhibits a strength of *c.* $19\,\text{kJ mol}^{-1}$. By contrast, in an H–O bond the covalent bond distance is approximately 1.0 Å and has a strength of $463\,\text{kJ mol}^{-1}$ ($1\,\text{kcal} = 4.184\,\text{kJ}$). Because the joined H_2O molecules must be aligned along the axes of their bonding orbital, hydrogen bonding causes H_2O molecules to exist in strongly ordered assemblies.

Pervasive hydrogen bonding is evident in all physical properties that reflect the strengths of association among H_2O molecules in both liquid water and ice. For example, liquid water has the highest heat capacity, heat of vaporization, surface tension, and dielectric constant (ion insulating capability) of all substances. In addition, the amount of heat necessary to go from the solid to the liquid phase is greater for water than for all substances except ammonia. The unusually high temperatures needed to melt ice and boil water relative to dihydrides of other elements in the oxygen family are not readily predictable by the usual method of extrapolating physical property trends as a function of molecular mass (Fig. 3.2). Clearly, hydrogen bonding makes H_2O a peculiar molecule. One oceanographically important outcome of hydrogen bonding is that water is excellent thermostating material. For example, 1 g of water absorbs over 3000 J of energy as it is heated from ice at $-50\,^\circ\text{C}$ to steam at $+150\,^\circ\text{C}$ (Fig. 3.3). The same amount of heat would raise the temperature of 10 g of granite (heat capacity $\approx 0.8\,\text{J g}^{-1}$) to over 380 °C. This difference

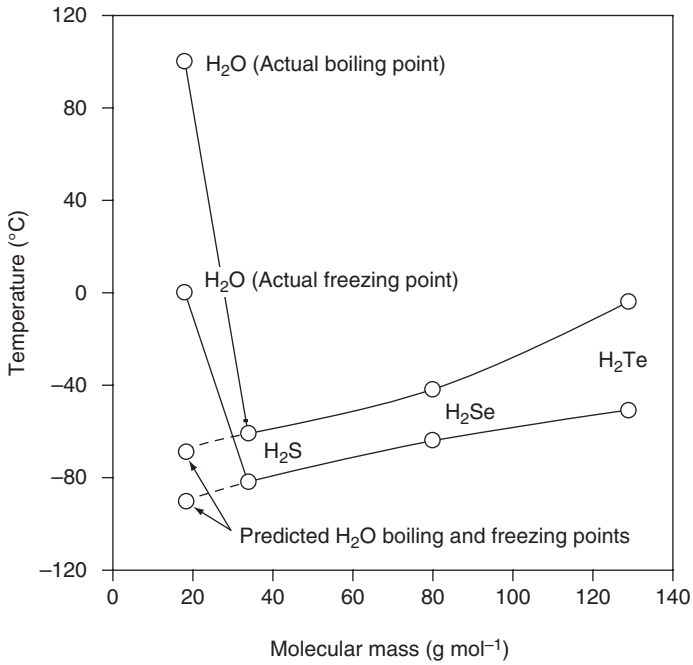


Figure 3.2. Freezing and boiling temperature of dihydride molecules of elements in column VI of the periodic table as a function of their molecular mass. The actual values for H_2O are connected by a solid line. Extrapolated melting and boiling points for water are indicated by the dashed line. Modified from Libes (1992).

Downloaded from https://www.cambridge.org/core. University of Hawaii at Manoa Library, on 09 Feb 2021 at 20:24:02, subject to the Cambridge Core terms of use, available at https://www.cambridge.org/core/terms. https://doi.org/10.1017/CBO9780511793202.004

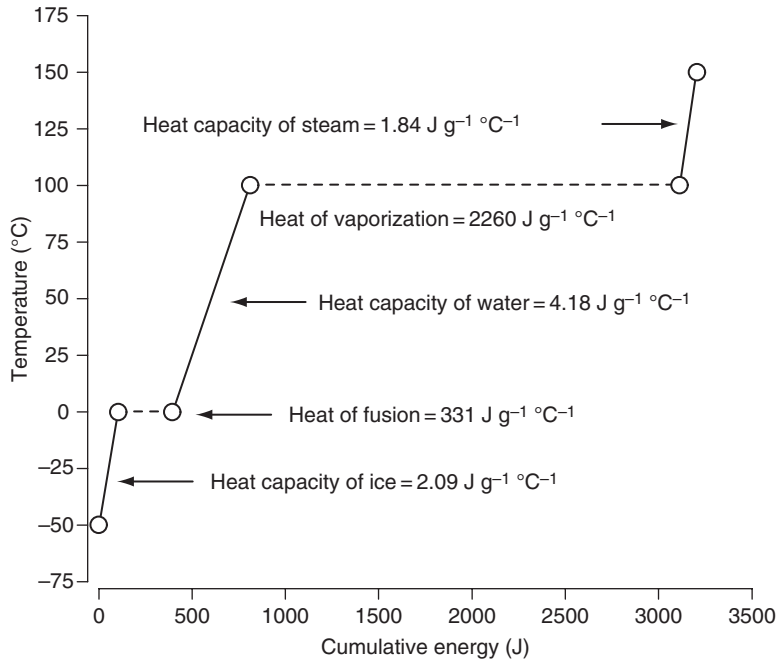


Figure 3.3. The cumulative heat energy needed to heat water from −50 to +150 °C. Modified from Libes (1992).

occurs largely because water has five times the heat capacity of granite and undergoes two (versus none for granite) phase transitions between −50 °C and +150 °C. It is easy to see why the sea is able to moderate temperature changes on adjacent continental margins and transport huge amounts of heat energy from low to high latitudes in the form of ocean currents and water vapor (Chapter 1).

The best defined structural properties of water are at the thermal extremes for vapor and ice. Water vapor consists primarily of individual H_2O molecules with negligible intermolecular attractions holding individual H_2O molecules together. Hence water vapor has essentially no structure. At the other temperature extreme, ice has a remarkably ordered structure. The structure of Ice-I, the stable form at atmospheric pressure, represents complete accommodation of individual molecules to maximal collective hydrogen bonding. In Ice-I (Fig. 3.4), all hydrogen atoms are located along the axes between the oxygen atoms of H_2O molecules that have been stretched into perfect tetrahedra. Full hydrogen bonding can be accomplished only by increasing the spacing of the water structural units in Ice-I, resulting in a solid of roughly half the density (0.92 g cm^{-3}) that would be exhibited for the closest packed structure (1.7 g cm^{-3}).

The specific structure of liquid water is poorly defined, but can be thought of as a slush of ice-like clumps floating in a pool of relatively unassociated H_2O molecules. This type of mixture helps explain many of the maxima and minima in such physical properties as density and viscosity that are often observed when liquid water is cooled or pressurized. The best known of these trends is the maximum in liquid water density near 4 °C (Fig. 3.5). This phenomenon

Downloaded from https://www.cambridge.org/core. University of Hawaii at Manoa Library, on 09 Feb 2021 at 20:24:02, subject to the Cambridge Core terms of use, available at https://www.cambridge.org/core/terms. https://doi.org/10.1017/CBO9780511793202.004

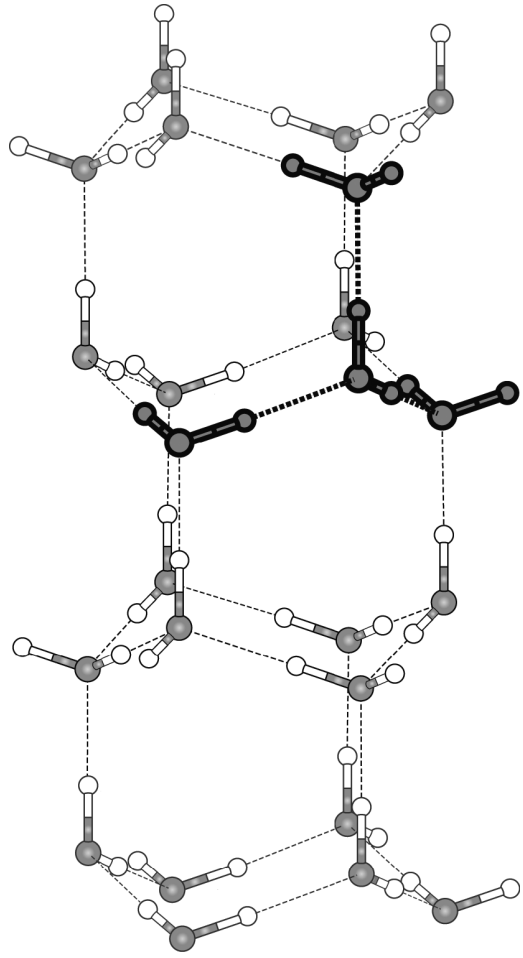


Figure 3.4. The structure of Ice-I, the predominant form of ice at one atmosphere pressure. Shaded spheres indicate oxygen atoms and open spheres hydrogen atoms. The darker shading represents four closest neighbor water molecules.

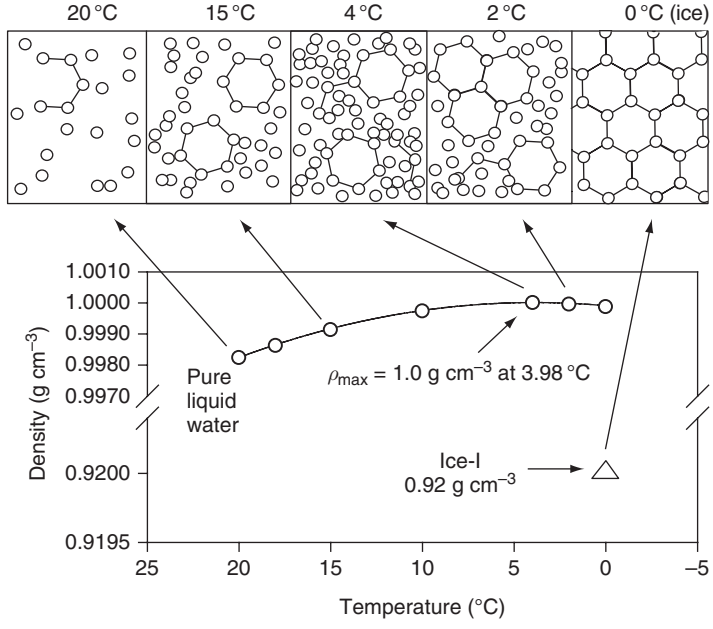


Figure 3.5 The density of liquid water as a function of temperature. The relative proportions of free molecules (unconnected circles) and ordered molecules (circles connected by lines) are illustrated for selected temperatures (°C) in the schematic illustration. Modified from Libes (1992).

Downloaded from https://www.cambridge.org/core. University of Hawaii at Manoa Library, on 09 Feb 2021 at 20:24:02, subject to the Cambridge Core terms of use, available at https://www.cambridge.org/core/terms. https://doi.org/10.1017/CBO9780511793202.004

apparently represents the net result of opposing density responses by associated and relatively free H_2O molecules to changing temperature. Lowering temperature toward the freezing point increases density by allowing slower-moving, free H_2O molecules to pack closer together, but will simultaneously decrease density through formation of more, less dense, ice-like clusters. These two opposing effects balance each other near 4 °C, below which the formation of ice-like structures predominates. Independent energy-related evidence for a high degree of association among H_2O molecules in the liquid state is that the amount of heat energy given off when liquid water freezes into ice (the heat of fusion) is only *c.*15% of the total that would theoretically be released by forming all the component hydrogen bonds from initially unassociated H_2O molecules. It is as if most liquid H_2O molecules were already in the frozen configuration. This high degree of structure in liquid water is not observed by most spectrographic-based measurements, which are too slow to resolve H_2O molecules as they rapidly interconvert between different association patterns.

3.1.2 Water–ion interactions

Given that H_2O molecules have strong dipoles, it is not surprising that they interact even more strongly with charged, dissolved ions than with each other. One of the most evident indications of this strong association is *electrostriction*, the reduction of water volume upon the addition of charged ions. This effect is illustrated in Table 3.1 for the addition of NaCl to water at concentrations similar to those in seawater. In this case, the total volume of the water–ion system shrinks by about 0.5% owing to the addition of *c.*3 wt% NaCl. This contraction results because H_2O molecules immediately surrounding the added ions are more closely packed than in bulk liquid owing to strong ion–dipole interactions (Fig. 3.6). The H_2O molecules of hydration will be packed with the negative (O) portions of the molecules oriented toward dissolved cations and the positive (H) regions directed toward dissolved anions. This reorientation capability partly nullifies the electrostatic charge of the hydrated ions and contributes toward the great ability of water to insulate, and hence dissolve, ions. Another common effect of dissolving salt in water is an increase in the viscosity of the solution, because the highly structured ion–dipole assemblies act as "lumps" that inhibit flow. The magnitudes of such electrostriction and viscosity effects increase with the charge density (charge/volume) and number of each type of dissolved ion. These effects are also a function of the temperature of the system. Because liquid water at higher temperatures has less structure, there is more potential for net structural increases as temperature increases. At low temperatures, large monovalent ions with low charge densities (e.g. K^+ and Cl^-) can act as "hydrogen bond structure breakers" because the electrostatic interaction with immediately adjacent H_2O molecules is greater than the strength of the hydrogen-bonded structure of pure water (Fig. 3.6).

Downloaded from https://www.cambridge.org/core. University of Hawaii at Manoa Library, on 09 Feb 2021 at 20:24:02, subject to the Cambridge Core terms of use, available at https://www.cambridge.org/core/terms. https://doi.org/10.1017/CBO9780511793202.004

Table 3.1. *Effects of ions on the density and structure of liquid water*

Ingredient	g	ρ (g cm^{-3})	cm^3
H_2O (25 °C)	970.78	0.993	973.5
NaCl	29.22	2.165	13.5
Simple sum	1000.00	—	987.0
Actual value	1000.00	—	982.0
Difference	0	—	5.0

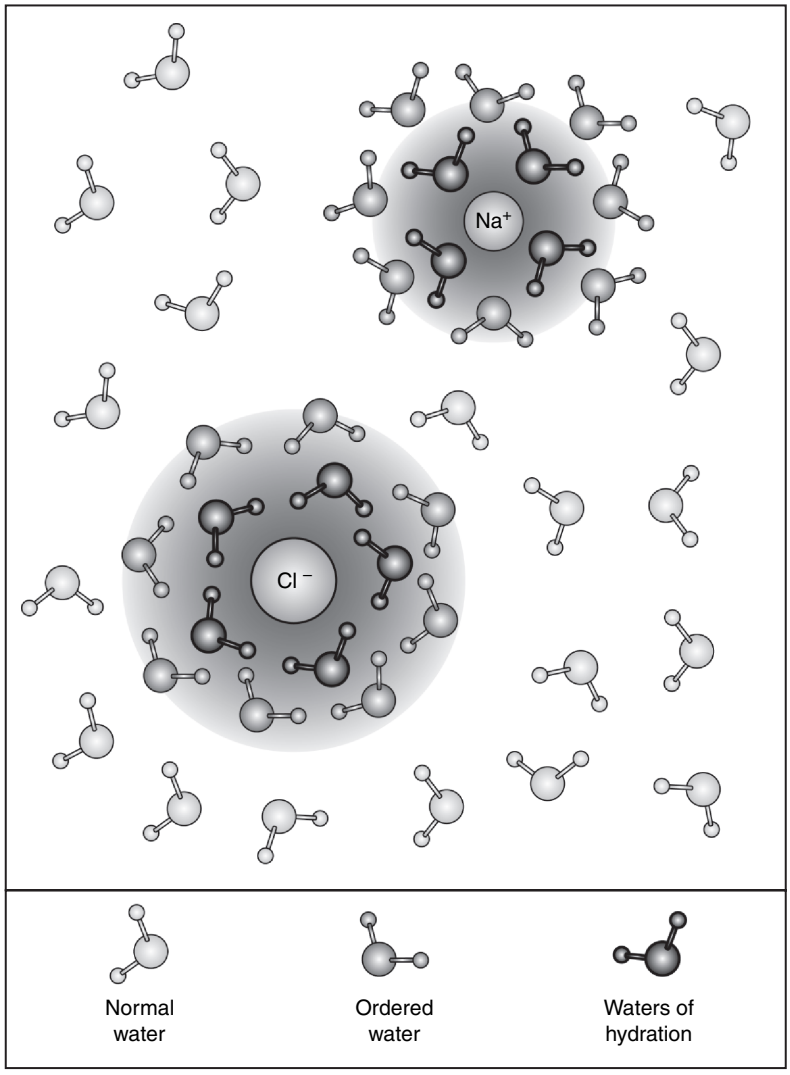


Figure 3.6. A cartoon of the structure of water in the vicinity of dissolved sodium and chloride ions. Waters of hydration are closest to the ions and indicated by the darkest water molecules. Layers of ordered water molecules outside the waters of hydration are indicated by shaded molecules.

Downloaded from https://www.cambridge.org/core. University of Hawaii at Manoa Library, on 09 Feb 2021 at 20:24:02, subject to the Cambridge Core terms of use, available at https://www.cambridge.org/core/terms. https://doi.org/10.1017/CBO9780511793202.004

3.2 | Ion–ion interactions and activity coefficients

In spite of the great insulating properties of water, ions still interact electrostatically with each other in aqueous solutions. The electrostatic force, F_z, between any two ions is expressed by the equation

$$F_z = \frac{Z_1 \times Z_2}{r^2}, \tag{3.1}$$

where Z_1 and Z_2 are the charges on the individual ions and r is the distance between them. In electrolytic solutions containing many ions, the average distance between ions decreases exponentially with their increasing concentration. Because ions interfere with each other in an electrolytic solution, their ability to react chemically is diminished except at infinite dilution, where large r values in the above equation drive F_z toward zero. In natural waters, containing finite concentrations of dissolved salts, an ion's *concentration* (amount per unit volume or mass) almost always overestimates its *activity* (reaction potential) versus conditions at infinite dilution. Thus, it is practical to have a correction factor that can be used to adjust the concentration of a dissolved substance, which is readily measured, to the corresponding chemical activity that actually expresses its reactivity. This correction factor is known as an *activity coefficient* (γ), and for any chemical species (i) is defined as

$$\gamma_i = \frac{a_i}{M_i} \tag{3.2}$$

where a_i and M_i indicate the activity and concentration of the ith species, respectively. In this book the chemical activities will usually be indicated within parentheses and concentrations within brackets, so that for sodium ion the relation between activity and concentration is written as

$$(Na^+) = \gamma_{Na^+}[Na^+]. \tag{3.3}$$

As discussed in Chapter 1, concentrations are normally expressed in the oceanographically convenient form of moles of solute per kilogram of solution (mol kg^{-1}) or in molar (M) units. Because activity coefficients are dimensionless correction factors, they are equally applicable to all concentration units.

3.2.1 Activity–ionic strength relations

The challenge of correcting concentrations to activities for natural waters is that the activity coefficients vary non-linearly, often in complex relations to bulk ion concentrations. For dilute electrolyte solutions, such as some lake and river waters, it is practicable to estimate the activity coefficient of an individual ion theoretically based on that ion's charge and a general measure of the effective total ion concentration of the bulk solution. The latter measure is called the *ionic*

Downloaded from https://www.cambridge.org/core. University of Hawaii at Manoa Library, on 09 Feb 2021 at 20:24:02, subject to the Cambridge Core terms of use, available at https://www.cambridge.org/core/terms. https://doi.org/10.1017/CBO9780511793202.004

Table 3.2. *Methods of calculating activity coefficients from ionic strength*

I is ionic strength in units of molarity, M. In the expressions, $A \approx 0.5$ in water at 25 °C, $B = 0.33$, and a is an adjustable parameter ranging from 3 to 9 (see Stumm and Morgan, 1996).

Approximation	Equation	I (M)
Debye–Hückel	$\log \gamma_i = -Az_i^2\sqrt{I}$	$<10^{-2}$
Extended Debye–Hückel	$\log \gamma_i = -Az_i^2 \frac{\sqrt{I}}{1+Ba\sqrt{I}}$	$<10^{-2}$
Davies	$\log \gamma_i = -Az_i^2\left(\frac{\sqrt{I}}{1+\sqrt{I}}\right) - 0.2I$	$<5 \times 10^{-1}$

strength, I, of the solution, which is simply half the sum of the molar, M, concentrations of each ion multiplied by its charge squared

$$I = \tfrac{1}{2}\sum M_i z_i^2. \tag{3.4}$$

(In older texts molality is used instead of molarity, but we adopt the modern convention of using the more environmentally familiar units.) Thus, a 1.0 M solution of NaCl has an I of 1.0 M, whereas a 1.0 M solution of $MgCl_2$ has an I of 3.0 M. Charges are squared in determinations of I because this parameter seeks to compensate for the electrostatic forces between ions that vary with charge squared (Eq. (3.1)). (This calculation for ionic strength is only exactly correct for the most dilute solutions, less than approximately 0.1 M. The calculation for more concentrated solutions is further complicated by incomplete dissociation and ion pairing; see later.) The ionic strength of seawater is $I \approx 0.7$.

The simplest expression relating the activity coefficient of a particular ion to the ionic strength of the solution is the Debye–Hückel equation (Table 3.2), which provides a useful approximation of γ_i at ionic strengths of $<10^{-2}$ M. The extended Debye–Hückel and Davies equations relate $\log \gamma_i$ to more complex expression of I and are useful for slightly more concentrated solutions (up to 0.1 M ionic strengths). All these equations are theoretically based and involve simplifying assumptions, such as treatments of ions as point charges (ignoring ionic dimensions), that fail at higher ionic strengths. Unfortunately, none of these equations can be applied at the ionic strength of seawater ($I \approx 0.7$ M), making other methods for calculating activity coefficients necessary.

3.2.2 The mean salt method

Single-ion activity coefficients at higher ionic strength are estimated by using an empirical approach in which complex ion and dipole interactions are accounted for by direct laboratory measurements. One such experimentally based approach that can be applied to seawater is the *mean salt method* (MSM). This procedure is based upon measurements

Downloaded from https://www.cambridge.org/core. University of Hawaii at Manoa Library, on 09 Feb 2021 at 20:24:02, subject to the Cambridge Core terms of use, available at https://www.cambridge.org/core/terms. https://doi.org/10.1017/CBO9780511793202.004

of the mean activity coefficients $\gamma_{\pm M_aX_b}$ of simple salt solutions that usually contain only two types of ion. For example, determination of the mean activity coefficient for the dissolution of a salt, M_aX_b,

$$M_aX_b \rightleftharpoons aM^{b+} + bX^{a-} \tag{3.5}$$

is done by measuring a property of the salt solution (e.g. electrical conductivity) that is known as a function of the salt activity and then comparing this with the value measured as a function of concentration. Another approach is to determine the activity of the ion in solution directly by using ion-sensitive electrodes.

The first step in the MSM is to measure the $\gamma_{\pm M_aX_b}$ of a KCl solution whose concentration is adjusted to be identical to the I of the electrolyte solution for which the activity coefficients are desired. For seawater a KCl solution of $I \approx 0.7$ would be used. One begins with KCl because the K^+ and Cl^- ions interact almost exclusively in an electrostatic manner, without formation of interfering ion pairs and other complexes. Next one assumes that $\gamma_{\pm M_aX_b}$ measured for any solution is the geometric mean of the individual activities of the component ions. The general formula for the geometric mean is

$$\gamma_{\pm M_aX_b} = \left[\gamma^a_{M^{b+}} \times \gamma^b_{X^{a-}}\right]^{1/(a+b)}, \tag{3.6}$$

which in the specific case of KCl becomes

$$\gamma_{\pm KCl} = \left[\gamma^1_{K^+} \times \gamma^1_{Cl^-}\right]^{1/2}. \tag{3.7}$$

It is further assumed that $\gamma_{K^+} = \gamma_{Cl^-}$, which simplifies Eq. (3.7) to

$$\gamma_{\pm KCl} = \gamma_{K^+} = \gamma_{Cl^-}. \tag{3.8}$$

This assumption is based on a variety of observations indicating that K^+ and Cl^- have similar effects on such properties of electrolyte solutions as viscosity and density. Once these two single-ion activity coefficients are established it is possible to make "bootstrap" estimates of the activity coefficients for all other ions by preparing simple solutions of individual salts containing either K^+ or Cl^- at the desired I. For example, to determine $\gamma_{Ca^{2+}}$, one would make up a $I = 0.7$ solution of $CaCl_2$, for which

$$\gamma_{\pm CaCl_2} = \left[\gamma_{Ca^{2+}} \times \gamma^2_{Cl^-}\right]^{1/3}. \tag{3.9}$$

Once $\gamma_{\pm CaCl_2}$ is determined experimentally, the only unknown would be $\gamma_{Ca^{2+}}$. For an anion, the same procedure would be followed by using a K salt. In this manner, single-ion activity coefficients can be determined for all the major ions in an electrolytic solution, such as seawater. In general, activity coefficients in seawater fall in the range of 0.6–0.8 for monovalent ions and 0.1–0.2 for divalent ions, and are near 0.01 for trivalent ions. Clearly, multiple charges lead to disproportionate attenuation of activity at a given electrolytic concentration, as would be expected given the strong dependency of electrostatic forces on charge (Eq. (3.1)).

Downloaded from https://www.cambridge.org/core. University of Hawaii at Manoa Library, on 09 Feb 2021 at 20:24:02, subject to the Cambridge Core terms of use, available at https://www.cambridge.org/core/terms. https://doi.org/10.1017/CBO9780511793202.004

Although useful, activity coefficients calculated by the MSM can only be applied under restricted conditions. One limitation is that empirically determined γ_i values hold only for the temperature, pressure and ionic strength of electrolyte solutions used in the laboratory measurements. A second complication for a mixed electrolyte like seawater is that γ_i values do not account for *ion pairing*. This term refers to a specific direct association of two ions that can occur in addition to general electrostatic interactions. An example of an ion pairing reaction that occurs in seawater is

$$Mg^{2+} + F^- \rightleftharpoons MgF^+. \tag{3.10}$$

The effects of this specific reaction would not be represented in MSM calculations. In fact, it is assumed that no ion pairs are formed at $I = 0.7$ in the experiments with individual electrolytes used to calculate activity coefficients in the MSM. This is true mainly for salts of potassium and chlorine, which are the ones primarily used in the MSM calculations. Because any ions that join to form ion pairs in a mixed electrolyte solution are effectively removed from solution with respect to reaction potential, an accurate determination of the extent of ion pairing in addition to the "free" ion activity coefficient must be made to determine the "total" activity coefficient in seawater.

The percentage of the total concentration of a specific ion in seawater that is involved in ion pairs can be determined from thermodynamic equilibrium information and will be demonstrated later in the chapter. For now, suffice it to say that the individual ion concentration is determined by multiplying the total ion concentration by a fraction between 0 and 1.0 representing the total ion that is free of ion pairs. The product, $(\%\text{free}_i/100)\, M_i$, can then be multiplied by the *free ion activity coefficient* to determine the activity. In general form, the total correction equation is

$$a_i = (\%\text{free}_i/100) \times \gamma_i \times [\ ]_i = \gamma_{i,T}[\ ]_i \tag{3.11}$$

where the overall correction, $((\%\text{free}_i/100) \times \gamma_i)$, is frequently referred to as the *total activity coefficient*, $\gamma_{i,T}$. The two correction factors are kept separate here so that it is clear that both ion pairing and general electrostatic inhibition factors are being addressed.

3.3 Thermodynamic basics

After chemical concentrations are converted to activities, the latter can be used to predict the probabilities and extents of specific chemical reactions based on the concept of *free energy*, the energy available in a chemical system to do work. This thermodynamically based method is founded on energetic relations that can be established for a chemical species or reaction system. The fundamental energetic property of a given chemical species is its *standard free energy of*

Downloaded from https://www.cambridge.org/core. University of Hawaii at Manoa Library, on 09 Feb 2021 at 20:24:02, subject to the Cambridge Core terms of use, available at https://www.cambridge.org/core/terms. https://doi.org/10.1017/CBO9780511793202.004

Table 3.3. | ΔG_f^0 *values of different forms of hydrogen*

Compound	ΔG_f^0 (kJ mol^{-1})
H_2 (gas)	0
H_2 (aqueous)	17.57
H^+ (aqueous)	0
H_2O (liquid)	−237.18
H_2O (gas)	−228.57

From Stumm and Morgan (1996).

formation (the symbol used in modern texts is ΔG_f^0), where the superscripted zero indicates the standard state and the subscript *f* indicates free energy of formation. By definition, ΔG_f^0 is the free energy change when one mole of a substance in its standard state is formed from stable elements under standard conditions.

All free energy changes are relative to each other and rely on definitions of values at *standard conditions* and *standard states*. These states are largely a matter of convenience, with *standard conditions* corresponding to the temperature and pressure occurring in a laboratory. *Standard states* correspond either to pure substances or to gas and liquid activities that are readily recreated and mathematically convenient. There are three important conventions to be observed: (1) *standard conditions* are set to 1 atm of pressure and 25 °C; (2) the *standard states* of dissolved ions, as well as pure solids, liquids, gases, and solutions have activities equal to 1; and (3) by definition, the ΔG_f^0 values at standard conditions for pure elements in their most stable forms, as well as the proton (H^+) and electron (e^-), are all equal to zero. The standard free energies of formation for various physical states of hydrogen and its oxide, water, are presented in Table 3.3. Note that ΔG_f^0 values vary with physical as well as chemical form, and normally only the pure element has a value of zero.

The usual unit of ΔG_f^0 is kilojoules per mole (kJ mol^{-1}). Tables of standard free energies of formation are collected in books with compilations of thermodynamic data (see, for example, Stumm and Morgan, 1996; Morel and Herring, 1993; *Handbook of Chemistry and Physics*, 1970).

3.3.1 Free energy change during reaction

The purpose of defining standard free energies of formation is to use these individual reference values to determine standard free energies of reaction, ΔG_r^0, where the subscript *r* indicates reaction. By definition, ΔG_r^0 is the free energy *change* attending a balanced chemical reaction that involves substances at their standard states

$$\Delta G_r^0 = \sum n\left(\Delta G_f^0\right)_{\text{products}} - \sum n\left(\Delta G_f^0\right)_{\text{reactants}}, \tag{3.12}$$

Downloaded from https://www.cambridge.org/core. University of Hawaii at Manoa Library, on 09 Feb 2021 at 20:24:02, subject to the Cambridge Core terms of use, available at https://www.cambridge.org/core/terms. https://doi.org/10.1017/CBO9780511793202.004

where n represents stoichiometric coefficients. Thus, for a generalized reaction (at standard conditions)

$$bB + cC \rightleftharpoons dD + eE \tag{3.13}$$

$$\Delta G_r^0 = d\Delta G_{f,D}^0 + e\Delta G_{f,E}^0 - b\Delta G_{f,B}^0 - c\Delta G_{f,C}^0. \tag{3.14}$$

Establishing ΔG_r^0 for a specific reaction of constituents in their standard states is a useful step toward developing a general expression for the free energy of reaction, ΔG_r, at *any* combination of reactant and product activities. The general expression relating the free energy of reaction to the activities of the reactants and products is

$$\Delta G_r = \Delta G_r^0 + RT \ln \frac{(D)^d (E)^e}{(B)^b (C)^c}, \tag{3.15}$$

where $R = 0.008\,314\,\text{kJ mol}^{-1}\,\text{deg}^{-1}$ and T is temperature in Kelvin [K = °C + 273.15]. Converting the natural logarithm to a base ten logarithm ($\ln(z) = 2.30 \log_{10}(z)$) gives

$$\Delta G_r = \Delta G_r^0 + 2.30RT \log_{10} \frac{(D)^d (E)^e}{(B)^b (C)^c}. \tag{3.16}$$

The quotient of activities in Eq. (3.15) is referred to as the *ion activity product*, Q, and is the only variable (at a fixed temperature and pressure) that determines ΔG_r. Note that if the activities of all the reactants and products in Eq. (3.16) are equal to unity, then $Q = 1$ and the last term becomes zero. Under these conditions, $\Delta G_r = \Delta G_r^0$, which makes sense because the standard state is defined as involving all chemical species at unit activity. Although activities of pure solids are always equal to unity regardless of the amount present in the chemical system, this is not true for gases (even if pure) and aqueous chemical species. Gas activities, called *fugacity* (see later), are presented in units of pressure, whereas activities of dissolved chemical species are given in units such as moles of solute per liter (or kilogram) of solution. In both cases, measured concentrations have to be corrected to corresponding activities by using the appropriate activity coefficients.

3.3.2 Thermodynamic equilibrium

Thermodynamic equilibrium is by definition the state of minimal free energy for a reaction system at a given temperature and pressure. Under these conditions $\Delta G_r = 0$ and no free energy is available in the system to do work. It follows from Eq. (3.16) that at equilibrium

$$\Delta G_r^0 = -2.30RT \log_{10} \frac{(D)^d (E)^e}{(B)^b (C)^c}. \tag{3.17}$$

Since ΔG_r^0, R and T are constants at any given temperature, so is Q. Thus, in the particular case of equilibrium, Q is equal to a fixed value that is referred to as the *thermodynamic equilibrium constant* (K). Therefore it follows by identity that

Downloaded from https://www.cambridge.org/core. University of Hawaii at Manoa Library, on 09 Feb 2021 at 20:24:02, subject to the Cambridge Core terms of use, available at https://www.cambridge.org/core/terms. https://doi.org/10.1017/CBO9780511793202.004

Table 3.4. | *ΔG_r, Q, K, and Ω values before, at, and after thermodynamic equilibrium*

State	ΔG_r	Q vs. K	Ω	Prediction
Before equilibrium	< 0	$Q < K$	< 1	Reaction *might* occur as written
At equilibrium	0	$Q \equiv K$	1	No net reaction can occur
After equilibrium	> 0	$Q > K$	> 1	Reaction cannot spontaneously occur as written

$$\Delta G_r^0 = -2.30RT \log_{10} K. \tag{3.18}$$

At 25 °C (298.15 K), Eq. (3.18) becomes

$$\Delta G_r^0 = -5.70 \times \log_{10} K. \tag{3.19}$$

Note that even though K is a constant in Eqs. (3.18) and (3.19), the individual activities of D, E, B, and C can vary. The major advantage of these equations is that the K for any balanced chemical reaction can be directly calculated from ΔG_r^0, which in turn can be determined by plugging ΔG_f^0 values from thermodynamic tables into Eq. (3.14). In a chemical system at equilibrium the individual activities of reactants and products are closely constrained by this equation.

The sign alone of ΔG_r is a useful indicator of whether a specific chemical reaction can spontaneously occur (i.e. without addition of free energy) in the direction *as written*. The reaction direction that is being tested must be clearly defined because it determines which expressions occur in the numerator and denominator of Q, and hence the sign of ΔG_r. Given this constraint, a negative ΔG_r value indicates that the reaction can occur spontaneously as written, whereas a positive sign indicates that the spontaneous reaction of reactants to products is energetically impossible. A ΔG_r value of zero indicates that the chemical system is in a state of *equilibrium*, where no free energy is available and no *net* reaction possible. The *reaction quotient*, Ω, is defined as Q/K and is helpful in indicating whether there is a deficit ($\Omega < 1$) or surplus of reactants versus products in a chemical system. These three conditions of ΔG_r, and the corresponding relationships of Q, K, and Ω, are summarized in Table 3.4. The main caveat to keep in mind when making predictions for the feasibility of a chemical reaction is that a thermodynamically favored reaction may not in fact occur because of unfavorable reaction kinetics that are not predictable. Thus the most definitive application of ΔG_r is to identify chemical reactions that cannot occur spontaneously as written at the given reactant and product activities.

Free energy relations are illustrated in terms of reaction extent in Fig. 3.7 using the same generalized reaction of B and C to form D and E as in Eq. (3.13). Equation (3.16) can be rewritten in parallel construction as a function of K and Q:

Downloaded from https://www.cambridge.org/core. University of Hawaii at Manoa Library, on 09 Feb 2021 at 20:24:02, subject to the Cambridge Core terms of use, available at https://www.cambridge.org/core/terms. https://doi.org/10.1017/CBO9780511793202.004

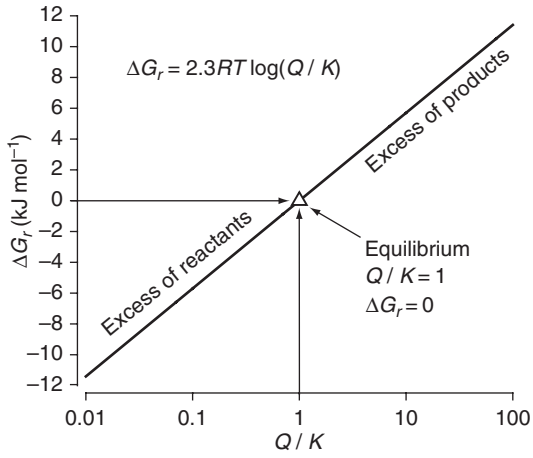


Figure 3.7. A schematic illustration of the change in free energy of a reaction, ΔG_r, as a function of the reaction progress. The *x*-axis is the quotient of the ion product, *Q*, and the equilibrium constant, *K*.

$$\Delta G_r = -2.30\ RT \log_{10} K + 2.30\ RT \log_{10} \frac{(\mathrm{D})^d (\mathrm{E})^e}{(\mathrm{B})^b (\mathrm{C})^c}. \tag{3.20}$$

The two terms to the right can be combined to generate the alternate form

$$\Delta G_r = 2.30\ RT \log_{10}(Q/K). \tag{3.21}$$

This relation is plotted in Fig. 3.7. Equilibrium ($\Delta G_r = 0$) corresponds to the point at which $Q = K$. Prior to equilibrium, there is a deficit of products versus reactants ($Q < K$) that corresponds to a negative ΔG_r and the potential to react until Q increases to equal K. If the system is in a state where $Q > K$ and ($\Delta G_r > 1$), reaction to the right will only increase Q and move the reaction system toward an even greater free energy excess versus the reference point of ΔG_r^0, so this cannot occur. Rather, the reaction is driven to the left until $Q = K$.

3.4 Equilibrium constraints on chemical activities

3.4.1 Speciation of ions in seawater

Because reactions among ionic species in solution are rapid, thermodynamic calculations are used to constrain the activities of dissolved chemical species at equilibrium. Garrels and Thompson (1962) were the first to calculate the speciation of the major ions in seawater by determining the extent to which each species is involved in ion pairing with each counter-ion. This information is necessary to establish the percentages of free major ions available in chemical equilibrium calculations. This section presents an example of how such multiple equilibrium systems can be constrained.

The example system consists of ions released by the complete dissolution of 1.00 mol each of $MgSO_{4(s)}$ and $CaF_{2(s)}$ in 1.00 l of solution at 25 °C and 1 atm of pressure, resulting in concentrations of total Mg, SO_4 and Ca of 1 molar, M, and total F of 2 M. The goal is to use

Downloaded from https://www.cambridge.org/core. University of Hawaii at Manoa Library, on 09 Feb 2021 at 20:24:02, subject to the Cambridge Core terms of use, available at https://www.cambridge.org/core/terms. https://doi.org/10.1017/CBO9780511793202.004

thermodynamic information to determine the concentrations of the four dissolved free ions, Mg^{2+}, Ca^{2+}, SO_4^{2-}, and F^-, plus all four dissolved ion pairs that they form, $MgSO_4^0$, MgF^+, $CaSO_4^0$, and CaF^+. We will assume that these ions form no precipitates or complexes in addition to simple ion pairs (meaning there are no entities like MgF_2^0 or CaF_2^0). Given that there are eight unknown concentrations, it will be necessary to generate eight independent equations describing the amounts and interactions of these ions. Half of the needed constraints can be derived from mass balance for concentrations of the four ions (excluding oxygen).

$$[Mg]_t = [Mg^{2+}] + [MgSO_4^0] + [MgF^+] \tag{3.22}$$

$$[Ca]_t = [Ca^{2+}] + [CaSO_4^0] + [CaF^+] \tag{3.23}$$

$$[SO_4]_t = [SO_4^{2-}] + [MgSO_4^0] + [CaSO_4^0] \tag{3.24}$$

$$[F]_t = [F^-] + [MgF^+] + [CaF^+]. \tag{3.25}$$

The other needed constraints can be obtained from equilibrium equations for the formation of each of the four ion pairs:

$$Mg^{2+} + SO_4^{2-} \rightleftharpoons MgSO_4^0 \tag{3.26}$$

$$Mg^{2+} + F^- \rightleftharpoons MgF^+ \tag{3.27}$$

$$Ca^{2+} + SO_4^{2-} \rightleftharpoons CaSO_4^0 \tag{3.28}$$

$$Ca^{2+} + F^- \rightleftharpoons CaF^0. \tag{3.29}$$

For example, the equilibrium constant for the formation of $[MgSO_4^0]$ can be determined by entering standard free energies of formation for Mg^{2+}, $MgSO_4^0$, and SO_4^{2-}, into Eq. (3.12) to obtain the standard free energy of the ion pair formation reaction, and then by using that ΔG_r^0 value in Eq. (3.18) to determine a $K_{MgSO_4^0} = 10^{2.36}$.

$$K_{MgSO_4^0} = \frac{(MgSO_4^0)}{(Mg^{2+})(SO_4^{2-})} = \frac{[MgSO_4^0]\gamma_{MgSO_4^0}}{[Mg^{2+}]\gamma_{Mg^{2+}}[SO_4^{2-}]\gamma_{SO_4^{2-}}}. \tag{3.30}$$

Note that single-ion activity coefficients are used to relate concentrations to the equilibrium constant. The only interactions inhibiting the activities of an ion and ion pair from achieving values equal to their concentration are the long-range charge interactions. In this calculation it is assumed for simplicity that the ions have the same single-ion activity coefficients as in seawater (see Table 3.5). Activity coefficients for neutral ion pairs are $\gamma = 1.13$, and values for singly charged ion pairs are similar to individually charged cations, $\gamma = 0.68$. Fluoride ion is assumed to have an activity coefficient equal to that of Cl^-, $\gamma_{F^-} = 0.63$. With the activity coefficients evaluated, one can determine the concentration ratio on the right side of Eq. (3.30):

Downloaded from https://www.cambridge.org/core. University of Hawaii at Manoa Library, on 09 Feb 2021 at 20:24:02, subject to the Cambridge Core terms of use, available at https://www.cambridge.org/core/terms. https://doi.org/10.1017/CBO9780511793202.004

Table 3.5. *Concentrations, single-ion activity coefficients, γ_i, percent of the ion that is free of ion pairing, and the total ion activity coefficient, $\gamma_{i,T}$, of the major seawater ions using the ion pairing model*

Ion	mol kg^{-1} [a]	γ_i	% free	$\gamma_{i,T}$
Na^+	0.4691	0.71	98	0.69
K^+	0.01021	0.63	98	0.62
Mg^{2+}	0.05282	0.29	89	0.26
Ca^{2+}	0.01028	0.26	88	0.23
Cl^-	0.54586	0.63	100	0.63
HCO_3^-	0.00186	0.68	79	0.54
SO_4^{2-}	0.02824	0.22	38	0.085
CO_3^{2-}	0.00023	0.21	14	0.029

From Millero (1996).
[a] Values are per kg of seawater.

$$\frac{[MgSO_4^0]}{[Mg^{2+}][SO_4^{2-}]} = \frac{(0.29)(0.22)}{1.13} \times 10^{2.36} = 12.9 \tag{3.31}$$

and therefore

$$[MgSO_4^0] = 12.9 \times [Mg^{2+}][SO_4^{2-}]. \tag{3.32}$$

The same procedure can be used to determine the concentrations of the other three ion pairs in terms of the known K for their formation and the concentrations of the two component ions

$$[MgF^+] = 10.2 \times [Mg^{2+}][F^-] \tag{3.33}$$

$$[CaSO_4^0] = 10.3 \times [Ca^{2+}][SO_4^{2-}] \tag{3.34}$$

$$[CaF^+] = 1.8 \times [Ca^{2+}][F^-]. \tag{3.35}$$

At this point, the above four equilibrium-based relations, Eqs. (3.32) to (3.35), and the four earlier mass balance relations, Eqs. (3.22) to (3.25), can be combined to give the following four equations, within which the unknown concentrations of the ion pairs have been eliminated:

$$[Mg]_t = [Mg^{2+}] + 12.9 \times [Mg^{2+}][SO_4^{2-}] + 10.2 \times [Mg^{2+}][F^-] = 1.0\,\text{M} \tag{3.36}$$

$$[Ca]_t = [Ca^{2+}] + 10.3 \times [Ca^{2+}][SO_4^{2-}] + 1.8 \times [Ca^{2+}][F^-] = 1.0\,\text{M} \tag{3.37}$$

$$[SO_4]_t = [SO_4^{2-}] + 12.9 \times [Mg^{2+}][SO_4^{2-}] + 10.3 \times [Ca^{2+}][SO_4^{2-}] = 1.0\,\text{M} \tag{3.38}$$

$$[F]_t = [F^-] + 10.2 \times [Mg^{2+}][F^-] + 1.8[Ca^{2+}][F^-] = 2.0\,\text{M}. \tag{3.39}$$

Downloaded from https://www.cambridge.org/core. University of Hawaii at Manoa Library, on 09 Feb 2021 at 20:24:02, subject to the Cambridge Core terms of use, available at https://www.cambridge.org/core/terms. https://doi.org/10.1017/CBO9780511793202.004

Because the numbers of unknowns and equations now are equal, the above equations can be solved for the four unknown ion concentrations. This can be done by iteration, where one makes an initial guess at the concentration of the anions F^- and SO_4^{2-} and then resets the concentration of free ion with successive loops. For more complicated systems a computer program to find the solution to simultaneous linear equations is more appropriate. The results for the free ions, $[Mg^{2+}] = 0.07$ M, $[Ca^{2+}] = 0.17$ M, $[SO_4^{2-}] = 0.30$ M and $[F^-] = 1.0$ M, and for the ion pairs, $[MgSO_4^0] = 0.26$ M, $[CaSO_4^0] = 0.52$ M, $[MgF^+] = 0.67$ M and $[CaF^+] = 0.31$ M, indicate that ion pairs dominate in this very concentrated solution and that the cations form ion pairs much more readily than anions.

Garrels and Thompson (1962) performed essentially the same calculation for the major ions in seawater. Their calculations were based on the assumption that the major ions in seawater associate only into ion pairs consisting of 1:1 cation : anion complexes. The activity coefficients used in this calculation and the resulting percentages of ion pairing (Table 3.5) have largely survived the test of time and can be broadly applied in thermodynamic descriptions of the major seawater ions and their reactions.

In complex electrolytes with relatively uniform major ion concentration, such as seawater, there are two commonly used types of equilibrium constant. In addition to the thermodynamic constant described above, apparent equilibrium constants, K', are often used. Apparent equilibrium constants are defined in terms of the *total concentrations* of chemical species. The apparent equilibrium expression for the reaction of A and B to give AB is

$$K' = \frac{[AB]_T}{[A]_T[B]_T}. \tag{3.40}$$

It follows that

$$K = \frac{\gamma_{T,AB}[AB]_T}{\gamma_{T,A}[A]_T\gamma_{T,B}[B]_T} = \frac{\gamma_{T,AB}}{\gamma_{T,A}\gamma_{T,B}} \times \frac{[AB]_T}{[A]_T[B]_T} = \frac{\gamma_{T,AB}}{\gamma_{T,A}\gamma_{T,B}} \times K', \tag{3.41}$$

where gammas, γ_T, are total activity coefficients that consider both electrostatic interactions and ion pairing. Although K and K' values for a given chemical reaction can be related by knowledge of the total activity coefficients of all chemical species involved, the advantage of apparent constants is that they can be determined experimentally in terms of concentrations and used without having to evaluate total activity coefficients. The disadvantage is that K' determined by experiment is valid only for the temperature, pressure and ionic composition of the experimental solution. Because the major ions in seawater have relatively constant concentrations, and highly complex interactions among themselves and with minor ions, equilibrium equations based on measured concentrations and apparent equilibrium constants are most often used in oceanography. This convention is used in the following chapter on

Downloaded from https://www.cambridge.org/core. University of Hawaii at Manoa Library, on 09 Feb 2021 at 20:24:02, subject to the Cambridge Core terms of use, available at https://www.cambridge.org/core/terms. https://doi.org/10.1017/CBO9780511793202.004

the carbonate system, but the subscript $_T$ on the concentration brackets, [ ], is deleted for convenience.

3.4.2 Equilibrium among coexisting phases: the phase rule

So far we have considered chemical equilibrium in solution only. The thermodynamic constraints can be applied to reactions among all phases, including gas partitioning between vapor and liquid phases, and reactions between solid and dissolved phases. A thermodynamically related tool for determining the quantitative constraints among phases in an equilibrium system is the *Gibbs phase rule*,

$$F = C + 2 - \bar{P}. \tag{3.42}$$

In this equation F represents the *degrees of freedom* within the system, that is the number of constraining independent variables such as concentrations, temperature, and pressure. $\bar{P}$ represents the *total number of phases* such as a gas, a homogeneous solution, or a homogeneous solid. Variable C corresponds to the *number of components* in the solution, which can be thought of as the minimal number of minerals, molecules and ions that are needed to fully create the mixture. In the previous ion pairing example, $C = 9$ (the eight different ions plus water), and $\bar{P} = 1$ (the homogeneous liquid solution without a gaseous phase being included), so that $F = 10$. If the temperature and pressure of the solution are fixed, F is reduced by two to a value of eight. This means that eight independent equations are necessary to fix each chemical component at a given activity (or concentration). In the previous ion pairing example, those constraints came from mass balance and equilibrium relations. Had another component, for example CaF_2^0, existed in appreciable amounts in the solution at equilibrium, the previous calculation results would have been in error. This problem could be addressed by using thermodynamic data to calculate the equilibrium constant for formation of CaF_2^0, which (along with the corresponding activity coefficient) would add the needed additional constraint. In effect, fixing the temperature and pressure of the system locks in the values of the equilibrium constants.

Another example that illustrates the constraining effect of adding additional phases is that for pure water. If only pure water is present in a system ($C = 1$) in only one phase (either solid, liquid or gas) ($\bar{P} = 1$), then $F = 1 + 2 - 1 = 2$. In this case, the two degrees of freedom are system temperature and pressure (T and P). When only one pure water phase is present, the system is confined only to T and P values within the liquid water region of the phase diagram (Fig. 3.8). If, however, the number of phases is increased to two, then only one degree of freedom remains. On the phase diagram for water, the simultaneous presence of two phases would constrain all T and P values to fall on one of the three lines separating the gas–liquid, gas–ice or ice–liquid regions. Along any of these lines, setting T fixes P and vice versa. If all three water phases are present at one time, the Gibbs phase rule indicates zero degrees of freedom, and hence fixes both T and P values. On the phase diagram, this unique

Downloaded from https://www.cambridge.org/core. University of Hawaii at Manoa Library, on 09 Feb 2021 at 20:24:02, subject to the Cambridge Core terms of use, available at https://www.cambridge.org/core/terms. https://doi.org/10.1017/CBO9780511793202.004

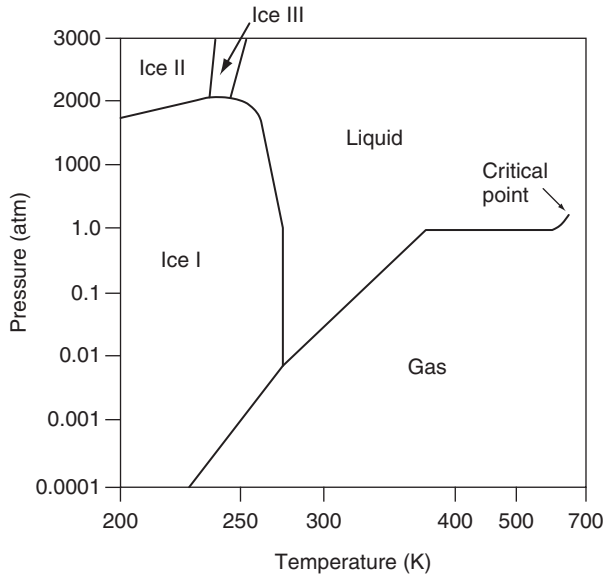


Figure 3.8. The phase diagram for pure water, demonstrating the relationships among the degrees of freedom in *T* and *P* space and the number of possible phases. See text.

circumstance corresponds to the triple point of water, which occurs at $T = 273.2$ K and $P = 0.006$ atm vapor pressure (Fig. 3.8).

3.4.3 Solid–solution equilibrium: $CaCO_3$

An example of how a free energy calculation can be used to predict whether a spontaneous reaction between a solution and solid phase is possible is the oceanographically important process of calcite ($CaCO_3$(s)) mineral dissolution. The question is whether this reaction

$$CaCO_3(s) \rightleftharpoons Ca^{+2} + CO_3^{2-} \tag{3.43}$$

is possible in warm surface seawater (1 atm and 25 °C). To address this question it is first necessary to look up ΔG_f^0 values for all three chemical species and calculate the corresponding ΔG_r^0. In this case

$$\begin{aligned} \Delta G_r^0 &= 1 \times \Delta G^0_{f,Ca^{2+}} + 1 \times \Delta G^0_{f,CO_3^{2-}} - 1 \times \Delta G^0_{f,CaCO_3(s)} \\ &= -553.54 - 527.9 + 1128.8 = +47.4\,\text{kJ}. \end{aligned} \tag{3.44}$$

Once this value of ΔG_r^0 is substituted into the equation for the free energy of reaction,

$$\Delta G_r = 47.4 + 5.70 \log_{10} \frac{(Ca^{2+})^1 (CO_3^{2-})^1}{(CaCO_3(s))^1}, \tag{3.45}$$

the only remaining unknowns are the activities of the three chemical species. These must be obtained from the corresponding concentrations, activity coefficients, and percentages of free ion in seawater (see Table 3.5). Because the activity of ($CaCO_3$(s)) is by definition equal to unity (assuming this solid mineral is pure), the denominator of *Q* in Eq. (3.45) drops out. At this point, the activities (calculated from the information in Table 3.5) can be substituted into Eq. (3.45) to give

Downloaded from https://www.cambridge.org/core. University of Hawaii at Manoa Library, on 09 Feb 2021 at 20:24:02, subject to the Cambridge Core terms of use, available at https://www.cambridge.org/core/terms. https://doi.org/10.1017/CBO9780511793202.004

$$\Delta G_r = 47.4 + 5.70 \log_{10}\left[\left(\frac{\%\text{free}}{100}\right)_{Ca^{2+}} \times \gamma_{Ca^{2+}} \times [Ca^{2+}] \times \left(\frac{\%\text{free}}{100}\right)_{CO_3^{2-}} \times \gamma_{CO_3^{2-}} \times [CO_3^{2-}]\right]$$
$$= 47.4 + 5.70 \log_{10}\left[\left(\frac{88}{100}\right) \times 0.26 \times 1.03 \times 10^{-2} \times \left(\frac{14}{100}\right) \times 0.21 \times 2.3 \times 10^{-4}\right]$$
$$= 47.4 + 5.70 \log_{10}(1.59 \times 10^{-8}) = 3.0 \text{ kJ mol}^{-1}. \quad (3.46)$$

Because ΔG_r is positive ($Q > K,\ \Omega > 1$), it is impossible that the reaction (Eq. (3.43)) will go spontaneously to the right and that calcite will dissolve in surface seawater under the specified conditions (coccolithophorides can relax). In fact, surface seawater has an excess of reactants versus the equilibrium point (Fig. 3.7) and is "supersaturated" with respect to calcite. Although the reverse reaction of calcite precipitation is energetically favorable, it too does not occur readily in surface seawater because of kinetic constraints.

3.4.4 Solid–solution adsorption reactions

Adsorption thermodynamics is distinct from the solid–solution reactions discussed previously or the solution–gas equilibrium reactions to be discussed in the following section because it deals with *exchange* equilibrium between ions in solution and on the solid surface, as opposed to *reaction* equilibrium between bulk phases. Adsorption of ions at solid surfaces plays an important role in controlling the concentration of trace metals in seawater. In fact, it has been suggested that surface adsorption reactions are the predominant mechanism controlling the chemistry of the sea (Whitfield and Turner, 1979; Li, 1981). There are several different models of the metal oxide surface. One of the most successful is the Stumm–Schindler model, in which the metal oxide surface in nature is treated with the same acid–base equilibrium equations used for solutions. This model (Fig. 3.9) envisions a metal oxide surface in which metal ions are partly coordinated, leaving a residual positive charge. H_2O molecules adsorb to the surface, orienting their more negative oxygen end toward the surface. Ultimately each H_2O molecule loses a proton by *dissociative chemisorption*, resulting in a hydroxylated surface (Fig. 3.9c). The result is that the surface, designated as $\equiv$S, is complexed by OH^- ions to form, $\equiv SOH_n$, which can exchange protons just like acids in water. The acid–base (*amphoteric*) character of the surface can then be described by the same equations used for acid–base behavior in solution (see Chapter 4):

$$\equiv SOH_2^+ \underset{\longleftarrow}{\xrightarrow{[K_{a,1}]^s}} \equiv SOH + H^+ \quad (3.47)$$

$$\equiv SOH \underset{\longleftarrow}{\xrightarrow{[K_{a,2}]^s}} \equiv SO^- + H^+. \quad (3.48)$$

Downloaded from https://www.cambridge.org/core. University of Hawaii at Manoa Library, on 09 Feb 2021 at 20:24:02, subject to the Cambridge Core terms of use, available at https://www.cambridge.org/core/terms. https://doi.org/10.1017/CBO9780511793202.004

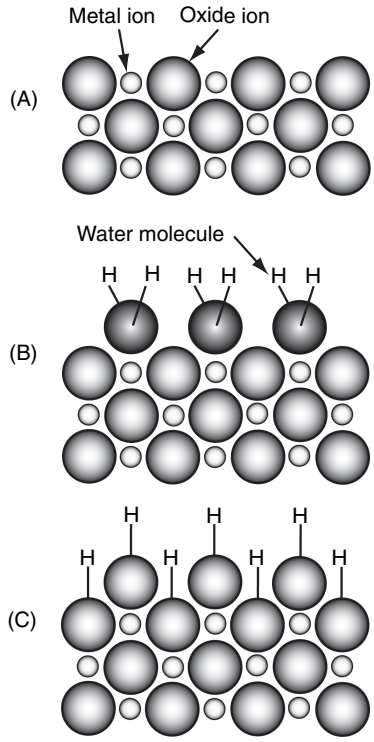


Figure 3.9. Illustration of the surface of a metal oxide where small circles are the metal atoms and large circles are oxygen atoms. (A) Surface metal atoms are not totally coordinated. (B) In water, surface metal ions coordinate water molecules. (C) Dissociative chemisorption leads to a hydroxylated surface. From Schindler and Stumm (1987).

Equilibrium constants for these reactions are indicated by *K*. The total capacity of the surface for adsorption of H^+ ions and the equilibrium constants are determined by potentiometric titration, which involves addition of a known amount of acid or base and then measuring the change in solution pH. The difference between the amount of titrant added and its concentration in the solution represents the amount of H^+ that has adsorbed onto, or reacted with, the surface.

It has been shown (Schindler and Stumm, 1987) that equilibrium constants characterizing the amphoteric behavior of metal oxides (the surface acidity) are linearly correlated with the equilibrium constants for the amphoteric behavior of the same metal ions in solution (acidity in solution). This finding supported the model in which the metal oxide surface is described with the same acid–base equations as the metal ions in solution, and allows the equilibrium constants for the oxide surfaces to be estimated from those determined in solution.

The next step in describing the importance of surface adsorption in this model involves the exchange affinity of the surface sites for metal ions as well as protons. In other words, metals in solution compete with protons for the oxide surface sites. Equations for this process are exactly analogous to those for similar solution reactions. Again it was demonstrated (see, for example, Schindler and Stumm, 1987) that the equilibrium constants determined for the competition between protons and metals for the metal oxide surface are linearly

Downloaded from https://www.cambridge.org/core. University of Hawaii at Manoa Library, on 09 Feb 2021 at 20:24:02, subject to the Cambridge Core terms of use, available at https://www.cambridge.org/core/terms. https://doi.org/10.1017/CBO9780511793202.004

correlated with the equilibrium constants describing the same reactions in solution. Further discussion of the adsorption model for oxide surfaces is beyond our purposes here and presented in elegant detail in books about aquatic chemistry (see, for example, Stumm and Morgan, 1996). These arguments are used later in the discussion of the dissolution rates of minerals (Chapter 9).

3.4.5 Gas equilibrium between the air and water

Thermodynamic equilibrium relations are used to define the partitioning of gases between the vapor and liquid phases. The amount of gas in the vapor phase is most often expressed as pressure (in units of atmospheres, bars or Pascals). One atmosphere is equal to 1013.25 millibars pressure (mbar) and 101.325 kilopascals (kPa; $1\,\text{bar} = 10^5\,\text{Pa}$). In a mixture of gases the *partial pressure*, p_i, of an individual gas, i, is its fraction of the total gas pressure. The total pressure of gases in the atmosphere, P_{atm}, is equal to the sum of the partial pressures of the individual gases

$$P_{\text{atm}} = p^{\text{a}}_{\text{N}_2} + p^{\text{a}}_{\text{O}_2} + p^{\text{a}}_{\text{H}_2\text{O}} + p^{\text{a}}_{\text{Ar}} + p^{\text{a}}_{\text{CO}_2} + \cdots \tag{3.49}$$

where the superscript $^{\text{a}}$ indicates atmosphere.

The *mole fraction*, X, of a gas in the atmosphere is defined as the number of moles of that gas per total moles of the atmospheric gases ($\text{mol}_{\text{g}}\,\text{mol}_{\text{a}}^{-1}$) in the absence of water vapor so that it does not depend on altitude. For an ideal gas the mole fraction and volume fraction are identical and the units are frequently presented as ($\text{cm}^3_{\text{g}}\,\text{m}_{\text{a}}^{-3}$) or parts per million by volume (ppmv). The atmospheric pressure and mole fraction of gas, C, are thus related by the partial pressure of water vapor, $p_{\text{H}_2\text{O}}$,

$$p^{\text{a}}_C = X_C \times (P_{\text{atm}} - p_{\text{H}_2\text{O}}). \tag{3.50}$$

In a dry atmosphere, the partial pressure and mole fraction are equal. Mole fractions for the major atmospheric gases are presented in Table 3.6, and the temperature dependence of $p_{\text{H}_2\text{O}}$ at equilibrium with seawater, $p^{\text{s}}_{\text{H}_2\text{O}}$, in Fig. 3.10. At saturation equilibrium, water vapor has the third highest partial pressure in the atmosphere.

The amount of gas that the solvent water will accommodate at thermodynamic equilibrium is represented by *Henry's Law*, in which the concentration in the water, C ($\text{mol}\,\text{kg}^{-1}\text{atm}^{-1}$) and *fugacity*, f, in the gas phase are related via the *Henry's Law coefficient*, K_{H} ($\text{mol}\,\text{kg}^{-1}\,\text{atm}^{-1}$),

$$C = K_{\text{H},C} \times f_C. \tag{3.51}$$

The fugacity and partial pressure of a gas are related in the same way as activities and concentrations in solution. Interaction of molecules with each other in a real gas diminishes the reactivity of an individual gas slightly, creating an effective partial pressure called the *fugacity*. As the gas pressure approaches zero, the pressure and fugacity are equal. The interference effect on gases in the atmosphere, however,

Downloaded from https://www.cambridge.org/core. University of Hawaii at Manoa Library, on 09 Feb 2021 at 20:24:02, subject to the Cambridge Core terms of use, available at https://www.cambridge.org/core/terms. https://doi.org/10.1017/CBO9780511793202.004

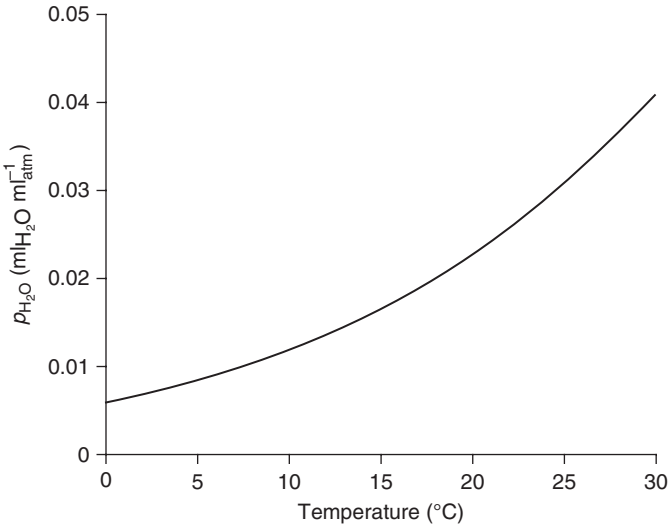


Figure 3.10. The partial pressure of water vapor in equilibrium with pure water as a function of temperature. From DoE (1994).

is much less than with ions in water. Except for CO_2, the fugacities of the major gases in the atmosphere are greater than 99.9% of their respective partial pressures. Klots and Benson (1963) suggest a value for $(f_i - p_i)/p_i$ for N_2 of 0.000 14–0.000 4 between 2 and 27 °C. Weiss (1974) calculates this value for CO_2 to be much larger but still less than 1%: 0.003–0.004 4 between 0 and 30 °C. For this reason fugacity and partial pressure tend to be used interchangeably for most atmospheric gases.

Interpreting the Henry's Law coefficient can be confusing because of the number of different units used in the literature. In this text it is presented in units of moles per kilogram so that the effect of pressure on volume in the ocean is normalized. Other units that are often used are molar (mol l^{-1}) and volume fraction at standard temperature (0 °C) and pressure (1 atm) (ml l^{-1}, STP). Be careful: STP for gases and "standard conditions" for free energies are not the same! The pressure terms are identical, but the temperatures are 0 and 25 °C, respectively. This is one of the casualties of an old science that evolved from many different laboratories. Since the volume of a mole of ideal gas at STP is exactly 22.414 l, there is a direct relation between moles of gas and milliliters (STP) of gas. Another potential confusion is that the Henry's Law relation is sometimes referred to as the reciprocal of the value given here, e.g. $1/K_H$. We can only say that the bulk of marine literature follows the definition used in Eq. (3.51), and one should make careful note of the units when using this constant.

Values of K_H in seawater at 20 °C and 1 atm are presented for several gases in Table 3.6. The values for the six most concentrated gases in the atmosphere were derived by using the regression equations presented in Table 3A1.1; others are taken from the literature. Note that the values of K_H are all within a factor of 10 of each other except for CO_2 and N_2O, which are much more soluble than the other gases.

Downloaded from https://www.cambridge.org/core. University of Hawaii at Manoa Library, on 09 Feb 2021 at 20:24:02, subject to the Cambridge Core terms of use, available at https://www.cambridge.org/core/terms. https://doi.org/10.1017/CBO9780511793202.004

Table 3.6. *Solubilities of the major atmospheric gases in seawater (s = 35) at one atmosphere pressure and 20 °C*

X_C is the mole fraction in a dry atmosphere (Glueckauf, 1951); $K_{H,C}$, the Henry's Law coefficient; C^s, the concentration in seawater at saturation equilibrium with the atmosphere. Saturation concentrations and Henry's Law coefficients for N_2, O_2, Ar, CO_2, Ne and He are calculated by using the equations in Table 3A1.1. Values for K_r, CH_4 and N_2O are from the compilation in Wanninkhof (1992). No correction was made here for the difference between the volume of the solvent and the solution in β and α (see text).

Gas	X_C	$K_{H,C}$	$C^{s\,a}$	β^b	α^c
	$(mol_g\ mol_{atm}^{-1})$	$(mol\ kg^{-1} atm^{-1})$	$(\mu mol\ kg^{-1})$	$(cm_g^3)/(cm_{sw}^{-3})$	
N_2	7.8084×10^{-1}	5.51×10^{-4}	4.21×10^{2}	1.27×10^{-2}	1.36×10^{-2}
O_2	2.0946×10^{-1}	1.10×10^{-3}	2.25×10^{2}	2.53×10^{-2}	2.71×10^{-2}
Ar	9.34×10^{-3}	1.21×10^{-3}	1.10×10^{1}	2.78×10^{-2}	2.98×10^{-2}
CO_2	3.65×10^{-4}	3.24×10^{-2}	1.16×10^{1}	7.44×10^{-1}	7.98×10^{-1}
Ne	1.818×10^{-5}	3.84×10^{-4}	6.83×10^{-3}	8.82×10^{-3}	9.47×10^{-3}
He	5.24×10^{-6}	3.29×10^{-4}	1.66×10^{-3}	7.47×10^{-3}	8.01×10^{-3}
Kr	1.14×10^{-6}	2.20×10^{-3}	2.44×10^{-3}	5.05×10^{-2}	5.42×10^{-2}
CH_4	1.6×10^{-6}	1.21×10^{-3}	1.89×10^{-3}	2.78×10^{-2}	2.97×10^{-2}
N_2O	5.0×10^{-7}	2.34×10^{-2}	1.14×10^{-2}	5.37×10^{-1}	5.77×10^{-1}

[a] $C^s = K_{H,i} f_C$; the fugacity is assumed equal to the partial pressure, p, except for CO_2.
[b] The Bunson coefficient, $\beta = K_H(RT_{STP})\rho$, where $R = 0.082\,057\,l\,atm\,deg^{-1}\,mol^{-1}$; $T_{STP} = 273.15$; ρ is the density of seawater (at 20 °C and 35 ppt, $\rho = 1.024\,8\,kg\,l^{-1}$).
[c] The Ostwald solubility coefficient, $\alpha = K_H\,RT\rho = \beta(T\,/\,T_{STP}) = \beta T\,/\,273.15$.

Equation (3.51) refers to the general relation between the fugacity of a gas in solution and its concentration. We give f a superscript, w, to indicate that it refers to the water phase.

$$[C] = K_{H,C} \times f_C^{w}. \tag{3.52}$$

The fugacity of a gas in water is usually calculated from measurements of the gas concentration by using the above relation. The concentration of a gas in surface waters is at solubility equilibrium with the atmosphere (saturation) when the fugacities of the atmosphere and water are equal

$$f^{a} = f^{w} \tag{3.53}$$

so that

$$C^{sat} = K_{H,C} \times f_C^{a}. \tag{3.54}$$

The superscript, sat, indicates that this is the concentration of the gas at saturation equilibrium with the atmosphere and has sometimes been called the air solubility (Weiss, 1971). Concentrations at saturation equilibrium with air are presented for the major atmospheric gases at 20 °C and 1 atm in Table 3.6.

Downloaded from https://www.cambridge.org/core. University of Hawaii at Manoa Library, on 09 Feb 2021 at 20:24:02, subject to the Cambridge Core terms of use, available at https://www.cambridge.org/core/terms. https://doi.org/10.1017/CBO9780511793202.004

The solubilities of gases are sometimes presented as the *Bunson coefficient*, β, or the *Ostwald solubility coefficient*, α. These values are directly related to the Henry's Law coefficient (see Table 3.6), but they present the solubility in units that have some advantages conceptually. The Bunson coefficient is defined as the volume of gas at STP dissolved in a unit volume of solvent at some temperature, T, when the total pressure of the gas and its fugacity are 1 atm. The Ostwald solubility coefficient is the same as the Bunson coefficient except that the gas volume is not at STP, but rather at the same temperature as the solvent water. These quantities represent equilibrium between the pure gas and water where the solvent and solute are presented in the same units. One can envision these constants as air–water partition coefficients for a pure gas at equilibrium with water, when the gas phase is one atmosphere and the gas and water reservoirs have equivalent volumes. Bunson and Ostwald solubility coefficients for the major atmospheric gases are presented in the last two columns of Table 3.6. At 20 °C, when overlying gas and liquid water phases have equal volumes, only about 1% of pure N_2 gas and 2%–3% of either Ar or O_2 gas exists in the water at equilibrium. The solubility of the rare gases in these units increases with molecular mass from 0.75% for He to 5% for Kr and brackets the values for the most abundant gases N_2 and O_2. The anomalies are CO_2 and N_2O. On an equal volume basis the amount of CO_2 residing in the water at 20 °C is about 80% of that residing in the atmosphere. (This is the value in the absence of chemical reaction with water.)

The only tricky thing about Bunson and Ostwald solubility coefficients is that they represent a volume of gas per volume of solvent (not solution). Because gases increase the volume of the solution when they dissolve into it, a correction has to be made for this difference. The correction is significant and on the order of 0.14% (Weiss, 1971). The values presented in Table 3.6 have not been corrected for this effect, and since this is a potential point of confusion, we will use the Henry's Law coefficient most often in this book.

The temperature dependences of the Henry's Law coefficients of the different gases listed in Table 3.6 are quite variable (Fig. 3.11). Helium, the least soluble noble gas, has very little solubility temperature dependence between 0 and 30 °C. On the other hand, Kr, the second most soluble of the non-radioactive noble gases, is much less soluble at higher temperatures. More details about gas solubilities are presented in the chapter on air–sea gas exchange (Chapter 10). Another notable aspect of the temperature dependence of the gas solubilities is that they are not linear. Thus, mixing between parcels of water of different temperatures at saturation equilibrium with the atmosphere results in a mixture that is supersaturated. This effect has been observed for noble gases in the ocean and may ultimately have a utility as a tracer of mixing across density horizons.

Downloaded from https://www.cambridge.org/core. University of Hawaii at Manoa Library, on 09 Feb 2021 at 20:24:02, subject to the Cambridge Core terms of use, available at https://www.cambridge.org/core/terms. https://doi.org/10.1017/CBO9780511793202.004

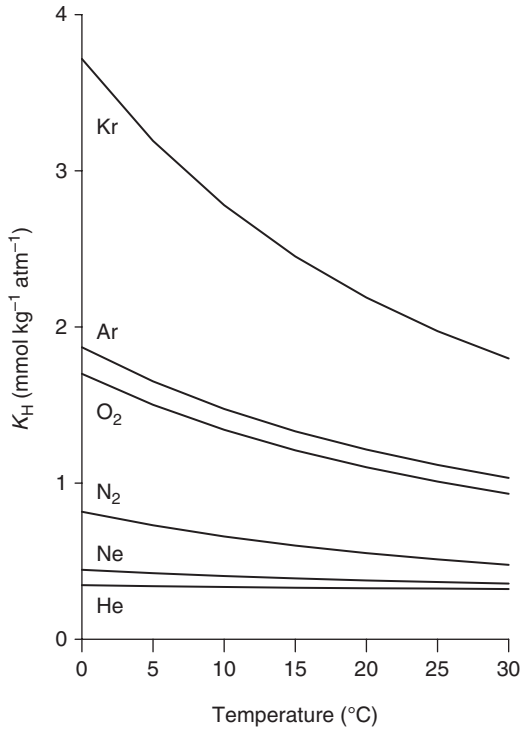


Figure 3.11. The Henry's Law coefficient, K_H (mol kg^{-1} atm^{-1}) for the noble gases, O_2 and N_2 in seawater (1 atm and $S = 35$) as a function of temperature. From the equations in Table 3A1.1.

3.5 Redox reaction basics

Chemical processes involving simultaneous *reduction* (electron gain) and *oxidation* (electron loss) are referred to as reduction–oxidation reactions, or *redox reactions* for short. Redox reactions are of wide interest because they include both photosynthesis and respiration and thus fuel essentially all life processes. Redox reactions are discussed here separately from other chemical reactions, because they involve an additional step in derivation of their free energy expression and are especially prone to slow approaches to equilibrium.

3.5.1 The standard electrode potential, E_h^0, and pe

A simple redox reaction in which dissolved copper-II ion is converted to elemental copper and elemental zinc is converted to the corresponding zinc-II cation is

$$Cu^{2+} + Zn^0 \rightleftharpoons Cu^0 + Zn^{2+}. \tag{3.55}$$

This complete reaction can be thought of as consisting of two simultaneous half-reactions

$$Zn^0 \rightarrow Zn^{2+} + 2e^- \tag{3.56}$$

$$Cu^{2+} + 2e^- \rightarrow Cu^0. \tag{3.57}$$

Downloaded from https://www.cambridge.org/core. University of Hawaii at Manoa Library, on 09 Feb 2021 at 20:24:02, subject to the Cambridge Core terms of use, available at https://www.cambridge.org/core/terms. https://doi.org/10.1017/CBO9780511793202.004

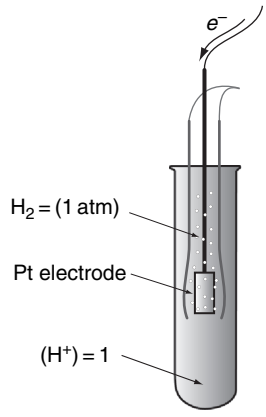


Figure 3.12. A schematic diagram of the Standard Hydrogen Electrode (SHE), which consists of a platinum electrode immersed in an aqueous solution at a pH of 1 in equilibrium with 1 atmosphere of hydrogen gas. The activity of H_2 is 1 atm and by convention the activity of $(H^+) = 1$.

In the first half-reaction Zn^0 loses electrons and by definition is oxidized. Note that the process of oxidation is defined in terms of electron loss, and does not necessarily involve the element oxygen in any form. In the second half-reaction Cu^{2+} accepts electrons and is said to be reduced. The two chemical species that make up each half-reaction are referred to as a *couple* (i.e. Zn^0/Zn^{2+} and Cu^{2+}/Cu^0) that interconvert by gain or loss of electrons. The separation of full redox reactions into half-reactions is largely conceptual because electrons are directly exchanged among reacting species and thus an oxidation cannot occur without a simultaneous reduction.

Nevertheless, it is convenient to be able to compare the relative affinities of redox couples for electrons as a tool for predicting reaction directions. This comparison is typically done by comparing the electron affinity of a couple to that of the Standard Hydrogen Electrode (SHE). As illustrated in Fig. 3.12, the SHE consists of a platinum electrode (redox reaction site) that is immersed in a water solution at 25 °C containing H^+ ions at an activity of 1 (pH = 0). Pure hydrogen gas is bubbled around the platinum electrode at a partial pressure of 1 atm, so that H_2 also has an activity of 1. The reaction occurring in the SHE is the reduction of H^+ to gaseous H_2:

$$2H^+ + 2e^- \rightleftarrows H_2\,(g). \tag{3.58}$$

By convention, the SHE is defined as having a *standard electrode potential*, E_h^0, of zero volts (V) at standard conditions (25 °C and 1 atm). The standard electrode potentials of other couples are similarly determined as reduction half-reactions at unit activity versus the SHE. If the E_h^0 for a given half-reaction is > 0, that couple has the potential to oxidize the SHE. A negative E_h^0 indicates a couple that can reduce the SHE. Tables of redox half-reactions and the corresponding E_h^0 values can be found in Stumm and Morgan (1996). Table 3.7 gives E_h^0 values and related parameters from these sources for a dozen environmentally important redox reactions.

The general free energy expression (Eq. (3.16)) can be extended to the description of redox reactions by establishing the relations between E_h^0 and ΔG_r^0. This can be done by the simple equation

$$\Delta G_r^0 = -nFE_h^0, \tag{3.59}$$

where ΔG_r^0 here is in joules (not kJ) and F is Faraday's constant (96 500 coulombs per mol) and equal to the electrical charge of one mole of electrons. The coefficient n represents the number of moles of electrons transferred in the balanced reaction. In essence, Eq. (3.59) can be thought of as representing the amount of free energy needed (or released) when nF electrons are passed through a standard electrode potential of E_h^0 for the couple in question. Dividing all terms in Eq. (3.15) by $-nF$ gives

$$-\frac{\Delta G_r}{nF} = -\frac{\Delta G_r^0}{nF} - \frac{RT}{nF} \times \ln \frac{(D)^d(E)^e}{(B)^b(C)^c}. \tag{3.60}$$

Downloaded from https://www.cambridge.org/core. University of Hawaii at Manoa Library, on 09 Feb 2021 at 20:24:02, subject to the Cambridge Core terms of use, available at https://www.cambridge.org/core/terms. https://doi.org/10.1017/CBO9780511793202.004

Table 3.7. *Common redox half-reactions and corresponding E_h^0, $E_{h,water}^0$, pe^0 and pe_{water}^0 [a] values*

Half-reaction	E_h^0	$E_{h,water}^0$ [a]	pe^0	pe_{water}^0
$\frac{1}{4}O_2(g) + H^+ + e^- \longrightarrow \frac{1}{2}H_2O$	+1.23	+0.81	+20.75	+13.75
$\frac{1}{5}NO_3^- + \frac{6}{5}H^+ + e^- \longrightarrow \frac{1}{10}N_2(g) + \frac{3}{5}H_2O$	+1.25	+0.75	+21.05	+12.65
$\frac{1}{2}MnO_2 + 2H^+ + e^- \longrightarrow \frac{1}{2}Mn^{2+} + H_2O$	+1.29	+0.46	+21.80	+7.80
$\frac{1}{2}NO_3^- + H^+ + e^- \longrightarrow \frac{1}{2}NO_2^- + \frac{1}{2}H_2O$	+0.84	+0.42	+14.15	+7.15
$\frac{1}{8}NO_3^- + \frac{5}{4}H^+ + e^- \longrightarrow \frac{1}{8}NH_4^+ + \frac{3}{8}H_2O$	+0.88	+0.36	+14.90	+6.15
$FeOOH(s) + 3H^+ + e^- \longrightarrow Fe^{2+} + 2H_2O$	+0.94	−0.30	+16.0	−5.0
$\frac{1}{2}CH_2O + H^+ + e^- \longrightarrow \frac{1}{2}CH_3OH$	+0.24	−0.18	+3.99	−3.01
$\frac{1}{8}SO_4^{2-} + \frac{9}{8}H^+ + e^- \longrightarrow \frac{1}{8}HS^- + \frac{1}{2}H_2O$	+0.25	−0.22	+4.25	−3.75
$\frac{1}{8}CO_2(g) + H^+ + e^- \longrightarrow \frac{1}{8}CH_4(g) + \frac{1}{4}H_2O$	+0.17	−0.24	+2.87	−4.13
$\frac{1}{6}N_2(g) + \frac{4}{3}H^+ + e^- \longrightarrow \frac{1}{3}NH_4^+$	+0.28	−0.28	+4.68	−4.68
$H^+ + e^- \longrightarrow \frac{1}{2}H_2(g)$	0.00	−0.41	0.00	−7.00
$\frac{1}{4}CO_2(g) + H^+ + e^- \longrightarrow \frac{1}{4}CH_2O + \frac{1}{4}H_2O$	−0.071	−0.48	−1.20	−8.20

[a] Values are calculated for unit activities of oxidant and reactant in neutral water of pH = 7.0 at 25 °C and 1 atm. Half-reactions are listed in order of decreasing pe_{water}^0, and hence of decreasing oxidizing power at pH 7. E_h values are in volts.

Substituting from Eq. (3.59) gives the electrode potential, E_h, counterpart of the free energy expression

$$E_h = E_h^0 - \frac{RT}{nF} \times \ln \frac{(D)^d (E)^e}{(B)^b (C)^c}. \tag{3.61}$$

At 25 °C and on a $\log_{10}$ basis, with $R = 8.314\,J\,mol^{-1}\,deg^{-1}$, the above expression becomes

$$E_h = E_h^0 - \frac{0.0592}{n} \times \log_{10} \frac{(D)^d (E)^e}{(B)^b (C)^c}. \tag{3.62}$$

Expressions (3.61) and (3.62) are different forms of the Nernst equation, which gives the electrode potential in volts of a *reduction* half-reaction as a function of E_h^0 for that reaction and the activities of the oxidized (reactants) and reduced (products) species raised to the power of their respective coefficients in the balanced redox equation. Note that if reactants and products were reversed (as is the case in some texts) the sign on the right side would be different. If the resulting E_h is equal to zero, there is no potential to do work and the system is at equilibrium. It then follows from Eq. (3.62) that

$$E_h^0 = \frac{0.0592}{n} \times \log_{10} K. \tag{3.63}$$

Standard electrode potentials can be calculated from the balanced half-reaction, thermodynamic tables of ΔG_f^0 (to yield ΔG_r^0) and Eq. (3.59). Equation (3.63) can then be used to determine the equilibrium constant for the half-reaction. In addition, the E_h^0 for a specific half-reaction can

Downloaded from https://www.cambridge.org/core. University of Hawaii at Manoa Library, on 09 Feb 2021 at 20:24:02, subject to the Cambridge Core terms of use, available at https://www.cambridge.org/core/terms. https://doi.org/10.1017/CBO9780511793202.004

be used in the Nernst equation, along with the activities of the various reactants and products, to determine the sign of the corresponding E_h and whether the reaction can occur spontaneously as written. A positive E_h corresponds to a negative ΔG_r (Eq. (3.59)), indicating the potential for a spontaneous reduction half-reaction (Table 3.7). The E_h for a particular half-reaction under natural conditions, however, may be quite different from those under standard conditions. This difference results primarily because environmental pHs are much higher than the value of 1 used to define standard conditions.

Since all redox reactions are written with equations that have electrons in them, one can think of the activity of the electron (e^-) as a master variable, just as the activity of the hydrogen ion (pH) is the master variable for acid–base (H^+ exchange) reactions (see Stumm and Morgan, 1996). An example is the reaction in the SHE (Eq. (3.58)):

$$E_h = E_h^0 - \frac{RT}{nF} \times \ln \frac{(H_2)^{1/2}}{(H^+)(e^-)}. \tag{3.64}$$

In the standard state the activities of H_2 and H^+ are one and at equilibrium $E_h = 0$, thus

$$\frac{E_h^0 F}{2.3RT} = -\log_{10}(e^-) = pe^0. \tag{3.65}$$

The above equation defines the *standard* p*e* (pe^0). The general expression for the generic reaction in Eq. (3.13) by analogy to Eq. (3.16) is

$$pe = pe^0 - \frac{1}{n} \log_{10} \frac{(D)^d (E)^e}{(B)^b (C)^c}. \tag{3.66}$$

This relation is useful because it defines the activity of electrons in the same manner as pH defines the activity of the H^+ ion. The two parameters, p*e* and pH, can be used as master variables to describe the stability of environmental reactions. Plots of p*e* versus pH are typically used to describe the environmental conditions within which specific chemical species are thermodynamically stable under a range of natural conditions (see, for example, Stumm and Morgan, 1996 and later discussion).

Redox conditions in aquatic systems are bounded by the reactions of potential electron donors and acceptors with water, much as water buffers acid/base reactions by accepting or donating protons (Chapter 4). For example, in oxic marine systems, where dissolved O_2 concentrations are measurable, the controlling redox couple (written as a reduction) is O_2–H_2O:

$$\tfrac{1}{2}O_2\ (g) + 2H^+ + 2e^- \rightleftharpoons H_2O. \tag{3.67}$$

The E_h^0 for this reaction is $+1.23$ V ($pe^0 = 20.8$). The E_h of this half-reaction in warm (25 °C) surface seawater can be calculated by plugging typical activity values into the Nernst equation (Eq. (3.62)). In this case the activity of H_2O would be 1.0 and the activity of dissolved O_2 would be approximately 0.2 atm. The latter value can be estimated

Downloaded from https://www.cambridge.org/core. University of Hawaii at Manoa Library, on 09 Feb 2021 at 20:24:02, subject to the Cambridge Core terms of use, available at https://www.cambridge.org/core/terms. https://doi.org/10.1017/CBO9780511793202.004

by assuming that the partial pressure of oxygen gas dissolved in surface seawater is equal to that in the atmosphere (by convention, gas concentrations are given in atmospheres and not moles). Surface seawater has a pH of ≈8 or an H^+ activity of $\approx 10^{-8}$ molar. Entering these values into the Nernst equation produces

$$E_h = E_h^0 - \frac{0.0592}{2} \times \log_{10} \frac{(H_2O)^1}{(O_2)^{1/2}(H^+)^2} \tag{3.68}$$

$$E_h = 1.23 - \frac{0.0592}{2} \times \log_{10} \frac{(1)^1}{(0.2)^{1/2}(10^{-8})^2} = 1.23 - 0.48$$
$$= +0.75 \text{ V}. \tag{3.69}$$

Note that the coefficients in reaction (3.67) could just as easily have been all divided by two to scale the stoichiometry to the exchange of a single electron (as is done in Table 3.7), without causing any change in the calculated E_h value. The E_h of water varies non-linearly with the concentration of oxygen and is not very sensitive to the O_2 concentration. For example, a 99% decrease in $[O_2]$ causes only a 4% drop in the E_h of the water. (Saturated water, 0.2 atm, has an E_h of 0.75 V; water with only 1% O_2 saturation, 0.002 atm, has an E_h of 0.72 V.) Thus, as long as measurable amounts of dissolved O_2 remain, the E_h of seawater will continue to be very positive.

The lower redox threshold for aqueous systems is also established by a gas-generating reaction involving a water constituent. In this case, the controlling half-reaction is the H^+–H_2 couple that also occurs in the SHE (Eq. (3.58)) and thus has an E_h^0 of zero. At this extreme, a stronger reducing agent (electron donor) than water will spontaneously convert protons to H_2 gas. Because the partial pressure of H_2 in the atmosphere is near zero, any generated hydrogen gas will tend to escape the liquid phase. As a simplification, and to include the fact that the partial pressure of O_2 in surface waters is roughly 0.2 atm, a concentration of one atmosphere is generally taken as the practical upper limit for both H_2 and O_2. At this partial pressure either gas forms bubbles and escapes, as occurs in electrolytic cells when strongly positive or negative voltages are introduced at platinum electrodes such as the SHE (Fig. 3.12).

Because each of the bounding redox reactions (3.58) and (3.67) involve H^+ as a reactant, this term shows up in the denominator of the Nernst equation (Eq. (3.62)) and therefore affects the E_h of both half-reactions, as is illustrated in Fig. 3.13. The three lines to the right in this figure indicate the atmospheres of O_2 present at equilibrium for different p*e* values at pH 4, 7, and 10. Similarly, the three lines to the left indicate the atmospheres of H_2 present at equilibrium that correspond to varying p*e* at the same three pH values. Beginning with the pair of lines for pH = 7 it can be seen that a p*e* greater than *c*.14 (an E_h greater than + 236 V; Eq. (3.65)) corresponds to more than 1 atm of O_2, which is an upper limit for oxidizing conditions. Likewise, a p*e* less than −7 (an E_h less than −118 V) is

Downloaded from https://www.cambridge.org/core. University of Hawaii at Manoa Library, on 09 Feb 2021 at 20:24:02, subject to the Cambridge Core terms of use, available at https://www.cambridge.org/core/terms. https://doi.org/10.1017/CBO9780511793202.004

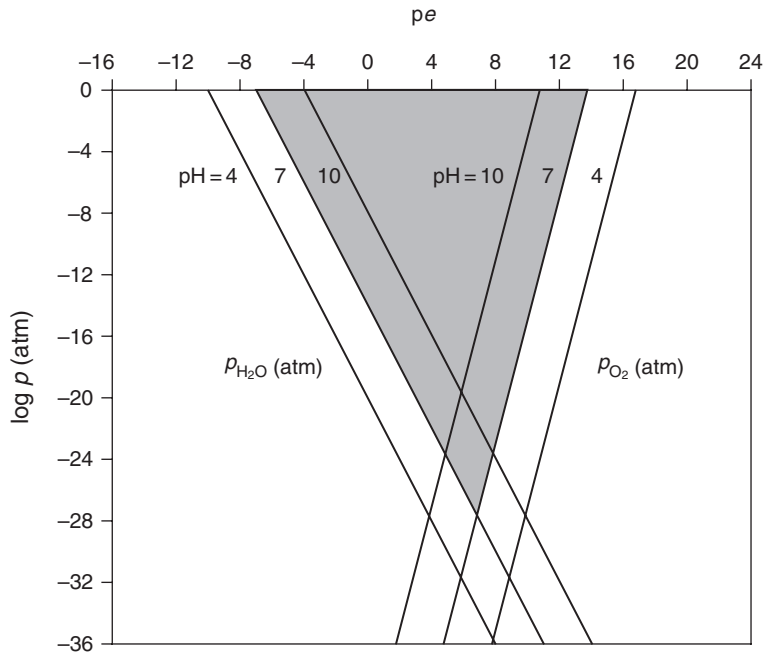


Figure 3.13. The log of the partial pressures of O_2 and H_2 as a function of pH for the half-reactions $\frac{1}{2}O_2 + 2H^+ + 2e^- = H_2O$ and $H^+ + e^- = \frac{1}{2}H_2(g)$, illustrating the field of pe that can be occupied by redox species in water at a given pH.

unstable at pH = 7 because of spontaneous evolution of H_2. The thermodynamic stability field for liquid water with respect to the two bounding redox reactions must fall in the wedge-shaped region between the two pH = 7 lines. For any chemical species to be thermodynamically stable in an aqueous system, the E_h for its half-reaction must fall within the stability field of water under the prescribed pH, T and P conditions.

3.5.2 Environmental redox reactions

What redox reactions occur in marine systems within the extremes of the oxygen and hydrogen gas evolution reactions? And what are the processes that determine the overall electron richness of a natural environment? To address these questions it is helpful to first consider the major source of redox imbalance at the Earth's surface, oxygenic photosynthesis, the simultaneous production of organic matter and O_2 gas by green plants. Although this process will be covered in much more detail within Chapter 6, the simplest chemical representation for photosynthesis is the unimolar equation

$$CO_2 + H_2O \rightleftarrows CH_2O(s) + O_2. \tag{3.70}$$

In this reaction solar energy captured by plants is used to "split water" and thereby produce organic matter (represented generically as $CH_2O(s)$) and molecular oxygen (O_2). These two products are, respectively, the most abundant reducing and oxidizing agents in the environment and have no other quantitatively important source in addition to photosynthesis.

Downloaded from https://www.cambridge.org/core. University of Hawaii at Manoa Library, on 09 Feb 2021 at 20:24:02, subject to the Cambridge Core terms of use, available at https://www.cambridge.org/core/terms. https://doi.org/10.1017/CBO9780511793202.004

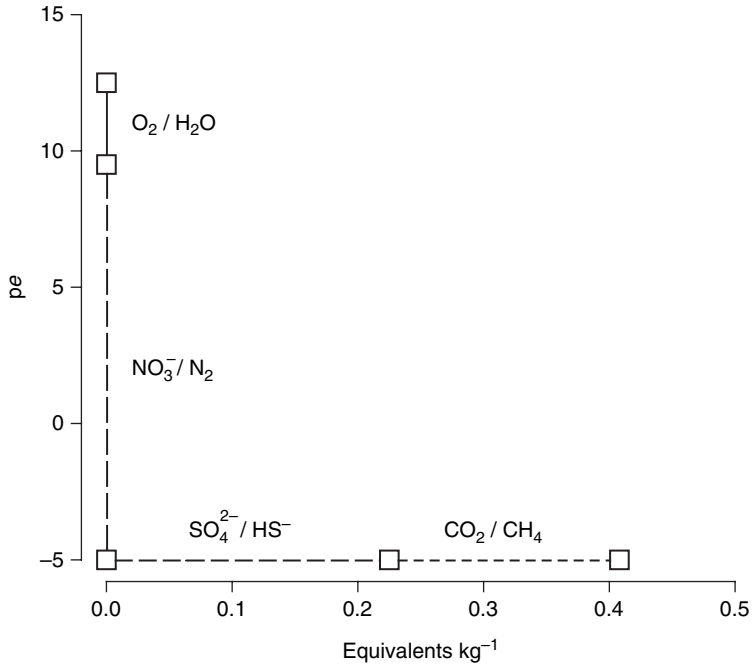


Figure 3.14. The redox buffering capacities of seawater illustrated by the ranges of pe in which electron acceptors are stable (ordinate) plotted against the concentration of the electron acceptor in seawater. Although O_2 and NO_3^- reduction dominate the redox reactions and the range of pe in seawater and sediments of the ocean, the most abundant electron acceptors are SO_4^{2-} and CO_2 and they occupy a relatively small range of pe.

The tendency is for organic matter produced by energy from the sun to break down into thermodynamically stable forms. The general pattern during the organic matter oxidation reaction is for electrons to pass from organic matter to the strongest oxidizing agent (electron acceptor) that is present at an appreciable concentration. Thus in general, electron acceptors will be utilized sequentially in the order of the corresponding half-reactions as listed in Table 3.7 (see also, Chapter 12). This is also the order of decreasing free energy yield, beginning with O_2 and then continuing with NO_3^-, $MnO_{2(s)}$, $FeOOH_{(s)}$, SO_4^{2-} and finally CO_2. Multicellular organisms are only capable of O_2-based respiration. The remaining oxidizing agents are exclusively utilized by microorganisms, many of which specialize in catalyzing only a particular redox reaction. The capacity of seawater constituents to serve as oxidizing agents can be assessed by multiplying their dissolved concentrations by the number of electrons that they take up during the conversion to their stable reduced forms. As is illustrated in Fig. 3.14, dissolved O_2 and NO_3^- have a very limited capacity for electrons before they are completely reduced to water and N_2 gas. In contrast, dissolved SO_4^{2-} ion and CO_2 have huge capacities for electrons.

Also illustrated in Fig. 3.14 is the constraint that as long as measurable amounts of O_2 and NO_3^- are present in seawater, the redox potential of the system will be poised near the very positive p*e* values (*c*.12.5) of the corresponding O_2–H_2O and NO_3^-–N_2 couples (see Table 3.7). When both oxidants are depleted, seawater cascades through trace levels of intermediate oxidizing agents to sulfate. The half-reaction that occurs at this point

Downloaded from https://www.cambridge.org/core. University of Hawaii at Manoa Library, on 09 Feb 2021 at 20:24:02, subject to the Cambridge Core terms of use, available at https://www.cambridge.org/core/terms. https://doi.org/10.1017/CBO9780511793202.004

$$SO_4^{2-} + 9H^+ + 8e^- \rightarrow HS^- + 4H_2O \tag{3.71}$$

has an E_h^0 of + 0.25 V. The E_h (and hence pe) of seawater at this redox stage can be estimated by the Nernst equation, which for reaction (3.71) becomes

$$E_h = E_h^0 - \frac{0.0592}{8} \times \log_{10} \frac{(HS^-)}{(SO_4^{2-})(H^+)^9}. \tag{3.72}$$

If it is assumed as a useful approximation that $[HS^-] = [SO_4^{2-}]$ and $\gamma_{SO_4^{2-}} = \gamma_{HS^-}$, then E_h becomes independent of the activities of the two sulfur species and

$$E_h = 0.25 - \frac{0.0592}{8} \times \log_{10} \frac{(1)^1}{(10^{-8})^9} = 0.25 - 0.53 = -0.28 \text{ V}. \tag{3.73}$$

The corresponding pe is $-0.28 \times F/2.3RT$ ($2.3RT = 16.9$ at 25 °C), or –4.7. Thus in going from control by the O_2–H_2O couple to the $SO_4^{2-}/SO_4^{2-}HS^-$ couple, seawater undergoes an abrupt decrease in redox potential of over 17 pe units – nearly the whole environmental range! Whether or not these couples actually control the pe or E_h of the environment depends on the lability of the electron transfer, which varies among chemical half-reactions (Stumm and Morgan, 1996).

This concept has been tested by measuring concentrations of redox couples in waters that transition from oxic (O_2-containing) to reducing (HS^--containing) conditions. An example is the water column of a fjord in Vancouver, BC, where water is trapped behind a sill and oxygen is totally depleted in the deeper waters. Depth profiles of seven redox couples measured simultaneously are plotted in Fig. 3.15, and pe values are calculated (Table 3.8) from thermodynamic data and the concentrations of the redox species in the 125–135 m depth range by using Eq. (3.66). The calculated pe ranges from 12.6 to −3.5 over the very short distance of a few meters. If the environment were in chemical equilibrium one would expect the values to be equal to the predominant (most concentrated) redox couples in the water, which are O_2–H_2O for the oxic layer and HS^-–SO_4^{2-} for the deeper reducing waters. To a first approximation the calculated pe values for SO_4^{2-} and Fe^{2+} are in the same range; however, this is not the case for the rest of the couples, which vary from 6.6 to 12.6. The main reason for the wide range of pe values in the more oxidizing waters is that the rates of oxidation of reduced species (Fe^{2+}, Mn^{2+}, Cr(III) and I^-) are slow compared with transport. These species are produced in the reducing deep waters and they mix to shallower waters that contain oxygen and nitrate, where they persist even though they are thermodynamically unstable. This example illustrates that chemical species in the environment are often not at redox equilibrium.

Perhaps the most obvious example of redox thermodynamic disequilibrium in the environment is nitrogen gas in oxic surface

Downloaded from https://www.cambridge.org/core. University of Hawaii at Manoa Library, on 09 Feb 2021 at 20:24:02, subject to the Cambridge Core terms of use, available at https://www.cambridge.org/core/terms. https://doi.org/10.1017/CBO9780511793202.004

Table 3.8. p*e values calculated from the concentration of redox pairs in Saanich Inlet*

pe^0 values are from Table 3.7 or Emerson *et al.* (1979). Values of p*e* were calculated by using Eq. (3.66) and the concentrations of the redox couples in the 125–135 m depth range of Fig. 3.15. pH was 7.4, $[SO_4^{2-}]$ is 28 mmol kg^{-1}.

Reaction	pe^0	pe
$\frac{1}{4}O_2(g) + H^+ + e^- \longrightarrow \frac{1}{2}H_2O$	20.8	12.6
$\frac{1}{6}IO_3^-(g) + H^+ + e^- \rightarrow \frac{1}{6}I^- + \frac{1}{2}H_2O$	18.4	10.5
$\frac{1}{8}NO_3^- + \frac{5}{4}H^+ + e^- \longrightarrow \frac{1}{8}NH_4^+ + \frac{3}{8}H_2O$	14.9	5.7
$\frac{1}{2}MnO_2 + 2H^+ + e^- \longrightarrow \frac{1}{2}Mn^{2+} + \frac{1}{2}H_2O$	21.8	9.8
$\frac{1}{3}CrO_4^{2-} + 2H^+ + e^- \rightarrow \frac{1}{3}Cr(OH)_2^+ + \frac{2}{3}H_2O$	22.0	6.6
$\frac{1}{2}FeOOH(s) + 2H^+ + e^- \rightarrow \frac{1}{2}Fe^{2+} + H_2O$	8.25	−2.7
$\frac{1}{8}SO_4^{2-} + \frac{9}{8}H^+ + e^- \longrightarrow \frac{1}{8}HS^- + \frac{1}{2}H_2O$	4.25	−3.5

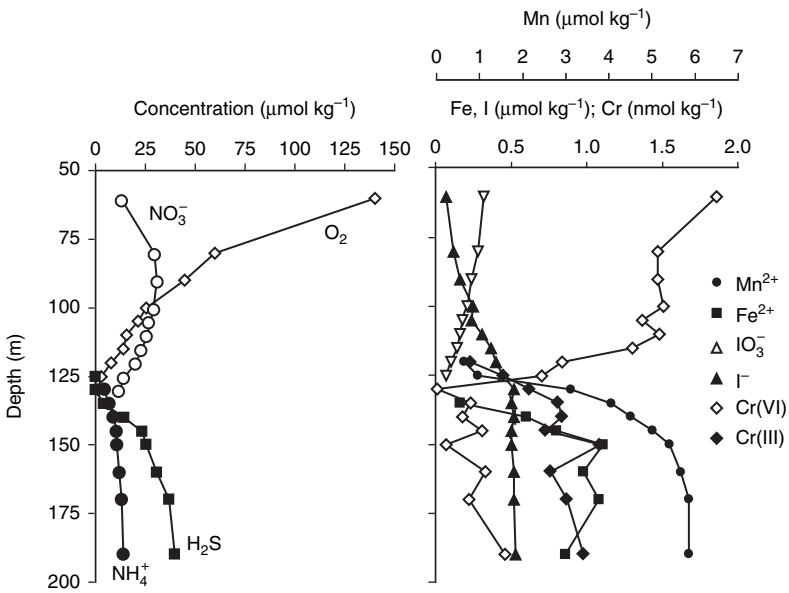


Figure 3.15. Concentrations of redox species (O_2, NO_3^-, NH_4^+, HS^-, Fe(II), Mn(II), IO_3^-, I^-, Cr(III) and Cr(VI)) with depth in the water column of Saanich Inlet, Vancouver, BC. The concentrations above and below the O_2–HS^- boundary are used to calculate the pe for each couple in Table 3.8. Modified from Emerson *et al.* (1979).

seawater. The reaction in question is listed on the second line of Table 3.7, which has an E_h^0 of +1.25 V and upon conversion to a non-fractional coefficient for NO_3^- becomes

$$NO_3^- + 6H^+ + 5e^- \longrightarrow \tfrac{1}{2}N_2 + 3H_2O. \tag{3.74}$$

If this half-reaction were at equilibrium with molecular oxygen in the atmosphere, then its E_h would be essentially the same as that of oxic seawater, which is +0.75 V. Plugging the appropriate terms for reaction (3.74) into the Nernst equation gives

Downloaded from https://www.cambridge.org/core. University of Hawaii at Manoa Library, on 09 Feb 2021 at 20:24:02, subject to the Cambridge Core terms of use, available at https://www.cambridge.org/core/terms. https://doi.org/10.1017/CBO9780511793202.004

Downloaded from https://www.cambridge.org/core. University of Hawaii at Manoa Library, on 09 Feb 2021 at 20:24:02, subject to the Cambridge Core terms of use, available at https://www.cambridge.org/core/terms. https://doi.org/10.1017/CBO9780511793202.004

Table 3A1.1. *Coefficients used in the fitting equations for air saturation (C^s) and Henry's Law coefficients (K_H) of gases in seawater (Table 3.6)*

The coefficients and fitting equations in the footnotes are for saturation values of O_2, N_2, Ar, Ne, and He in units of μmol kg^{-1} and ml kg^{-1}. Values can be transformed between these units by using the real gas molar volumes calculated from Van der Waals constants (22.385 9, 22.391 9, 22.386 9, 22.422 4 and 22.436 9 mol^{-1} for O_2, N_2, Ar, Ne, and He, respectively). The fitting equation for CO_2 is for the Henry's Law coefficient, K_H (mol kg^{-1} atm^{-1}) instead of the saturation concentration.

	O_2[a]	N_2[b]	Ar[b]	Ne[b]	He[c]	K_{H,CO_2}[d]
Coefficient		(μmol kg^{-1})		(nmol kg^{-1})	(ml kg^{-1})	(mol kg^{-1} atm^{-1})
A_0	5.808 710	6.432 41	2.791 63	2.181 40		
A_1	3.202 910	2.927 58	3.177 14	1.289 31	−67.217 8	−60.240 9
A_2	4.178 870	4.303 51	4.136 58	2.122 35	216.344 2	93.451 7
A_3	5.100 060	4.266 73	4.866 32		139.203 2	23.358 5
A_4	−0.098 664				−22.620 2	
A_5	3.803 690					
B_0	−0.007 016	−0.007 443 16	−0.006 963 17	−0.005 947 22		
B_1	−0.007 700	−0.007 999 36	−0.007 683 87	−0.005 093 70	−0.044 781	0.023 517
B_2	−0.013 86	−0.001 529 48	−0.001 190 78		0.023 541	−0.023 656
B_3	−0.009 515				−0.0034266	−0.0047035
C_0	$-2.759\,150 \times 10^{-7}$					
$[C]^s$ at 20 °C 35 ppt	225.5	420.5	11.08	6.826	3.729×10^{-5}	0.0324

[a] Garcia and Gordon (1992): $\ln C^s = A_0 + A_1T_s + A_2T_s^2 + A_3T_s^3 + A_4T_s^4 + A_5T_s^5 + S(B_0 + B_1T_s + B_2T_s^2 + B_3T_s^3) + C_0S^2$;
where $T_s = \ln\{(298.15 - t)(273.15 + t)^{-1}\}$ and t is temperature (°C).

[b] Hamme and Emerson (2004): same equation as in [a].

[c] Weiss (1971): $\ln C^s = A_1 + A_2(100/T) + A_3\ln(T/100) + A_4(T/100) + S\{B_1 + B_2(T/100) + B_3(T/100)^2\}$, where T is absolute temperature.

[d] Weiss (1974): $\ln K_{H,CO_2} = A_1 + A_2(100/T) + A_3\ln(T/100) + S\{B_1 + B_2(T/100) + B_3(T/100)^2\}$, where T is absolute temperature.

$$+0.75 = +1.25 - \frac{0.0592}{5} \times \log_{10} \frac{(0.2)^{1/2}}{(NO_3^-)(10^{-8})^6}. \quad (3.75)$$

Solving this equation (assuming concentrations equal activities) gives $\log (NO_3^-) = +5.3$, which is equivalent to $(NO_3^-) \approx 10^5$ M. Given the stoichiometry for the full oxidation reaction,

$$N_2 + 2.5O_2 + H_2O \longrightarrow 2HNO_3 \quad (3.76)$$

and the 4:1 molar excess of N_2 versus O_2 in the atmosphere (Chapter 1), it is apparent that the atmosphere would be stripped of essentially all oxygen before such a concentrated nitric acid solution could be formed. If this thermodynamically feasible reaction actually occurred, the ocean would become a highly oxidizing nitric acid bath in which carbon-based life forms would immediately perish. There would be no safety on land either in a thermodynamically spontaneous world because all organic matter would immediately combust to carbon dioxide and water. For living creatures and textbooks alike, slow kinetics in a thermodynamically imperfect world pose some distinct advantages.

References

DoE (1994) *Handbook of Methods for Analysis of the Various Parameters of the Carbon Dioxide System in Seawater*; version 2, ed. A. G. Dickson and C. Goyet. ORNL/CDIAC-74.

Emerson, S., R. Cranston and P. Liss (1979) Redox species in a reducing fjord: equilibrium and kinetic considerations. *Deep-Sea Res.* **1**, 26pp.

Garcia, H. E. and L. I. Gordon (1992) Oxygen solubility in seawater: better fitting equations. *Limnol. Oceanogr.* **37**, 1307–12.

Garrels, R. M. and M. E. Thompson (1962) A chemical model for sea water at 25 °C and one atmosphere total pressure. *Am. J. Sci.* **260**, 57–66.

Glueckauf, E. (1951) The composition of atmospheric air. In *Compendium of Meteorology*, Malone, T. F. (ed.), pp. 3–11. Boston, MA: American Meteorological Society.

Hamme, R. and S. Emerson (2004) The solubility of neon, nitrogen and argon in distilled water and seawater. *Deep–Sea Res*. I, **51**, 1517–28.

Handbook of Chemistry and Physics (1970) Cleveland, OH: The Chemical Rubber Publishing Co.

Klots, C. E. and B. B. Benson (1963) Solubilities of nitrogen, oxygen, and argon in distilled water. *J. Mar. Res.* **21**, 48–57.

Li, Y.-H. (1981) Ultimate removal mechanisms of elements from the ocean. *Geochim. Cosmochim. Acta* **45**, 1659–64.

Libes, S. M. (1992) *An Introduction to Marine Biogeochemistry*. New York, NY: John Wiley and Sons.

Millero F. (1996) *Chemical Oceanography*. Boca Raton, FL: CRC Press.

Morel, F. M. and J. G. Herring (1993) *Principles and Applications of Aquatic Chemistry*. New York, NY: Wiley Interscience.

Schindler, P. W. and W. Stumm (1987) The surface chemistry of oxides, hydroxides, and oxide minerals. In *Aquatic Surface Chemistry* (ed. W. Stumm), pp. 83–107. New York, NY: Wiley-Interscience.

Downloaded from https://www.cambridge.org/core. University of Hawaii at Manoa Library, on 09 Feb 2021 at 20:24:02, subject to the Cambridge Core terms of use, available at https://www.cambridge.org/core/terms. https://doi.org/10.1017/CBO9780511793202.004

Stumm, W. and J. J. Morgan (1996) *Aquatic Chemistry*. New York, NY: Wiley Interscience.

Wanninkhof, R. (1992) Relationship between wind speed and gas exchange over the ocean. *J. Geophys. Res.* **97**, 7373–82.

Weiss, R. F. (1971) The solubility of helium and neon in water and seawater. *J. Chem. Engin. Data* **16**, 235–41.

Weiss, R. F. (1974) Carbon dioxide in water and seawater: the solubility of a non-ideal gas. *Mar. Chem.* **2**, 203–15.

Whitfield, M. and D. R. Turner (1979) Water-rock partition coefficients and the composition of river and seawater. *Nature* **278**, 132–6.

Downloaded from https://www.cambridge.org/core. University of Hawaii at Manoa Library, on 09 Feb 2021 at 20:24:02, subject to the Cambridge Core terms of use, available at https://www.cambridge.org/core/terms. https://doi.org/10.1017/CBO9780511793202.004